Cement & Concrete Composites 33 (2011) 832–847

Contents lists available at ScienceDirect

Cement & Concrete Composites

journal homepage: www.elsevier.com/locate/cemconcomp

# Easy assessment of durability indicators for service life prediction or quality control of concretes with high volumes of supplementary cementitious materials

V. Baroghel-Bouny [a,*], K. Kinomura [a,b], M. Thiery [a], S. Moscardelli [c]

[a] Paris Est Univ. – French Institute of Science and Technology for Transport, Development and Networks (IFSTTAR, former LCPC) – Materials Department, Paris, France
[b] Taisei Corporation, Tokyo, Japan
[c] Laboratoire Régional des Ponts et Chaussées de l'Est Parisien, Le Bourget, France

ARTICLE INFO

*Article history:*
Received 24 December 2010
Received in revised form 26 April 2011
Accepted 29 April 2011
Available online 6 May 2011

*Keywords:*
Chloride diffusion coefficient
Durability indicator
Electrical resistivity
Liquid water permeability
Numerical inverse analysis
Supplementary cementitious material

ABSTRACT

This paper investigates whether durability indicators (DIs), more specifically transport properties, can be assessed by simple methods, e.g. direct experimental methods or indirect methods based on analytical formulas, for every type of concrete. First the results of electrical resistivity and *apparent* chloride diffusion coefficient obtained by direct measurement on a broad range of materials, particularly on high-volume supplementary cementitious materials (SCM) mixtures, are discussed. Then, various methods, in particular methods based on these last parameters, are compared for the assessment of *effective* chloride diffusion coefficient and "intrinsic" liquid water permeability, including for the latter a sophisticated method based on numerical inverse analysis. The good agreement observed between the various methods points out that simple methods can allow DI assessment with sufficient accuracy. Moreover, the available values of electrical resistivity, *effective*/*apparent* chloride diffusion coefficients and "intrinsic" liquid water permeability can be included in a database. Throughout the paper, the specificities of high-volume SCM mixtures are highlighted.

© 2011 Elsevier Ltd. All rights reserved.

## 1. Introduction

In recent years, sustainable development has become a major concern, in particular in the construction field [1,2]. In this context, a global approach is needed, in order to meet technical, economical, environmental and societal requirements in an optimized way for the whole life cycle of a concrete structure [3,4]. The task of designers, engineers and infrastructure owners is therefore now more complex. In particular, they need to combine improved durability and environmentally friendly materials and structures. From a (concrete) material point of view, they are thus interested, on the one hand in relevant parameters, which can characterize durability, and on the other hand in the use of wastes, by-products or recycled materials, which are, at least at present time, regarded as zero-$CO_2$ emission constituents. As a consequence and in order to make this task easier, there is an increasing demand to include in current concrete or design standards (e.g. EN 206-1 [5]) the advanced concepts of durability and service life (SL) prediction, including performance-based and/or probabilistic approaches (see e.g. [6]), in particular with respect to the prevention of steel corrosion in reinforced concrete (RC) structures.

In this context, a general approach based on so-called *durability indicators* (DIs), which are key material properties with regard to durability (e.g. porosity, permeability or diffusion coefficient), has been developed [3,7–9]. Note that other similar concepts can be found in the literature [10–13]. A system of classes of "potential" durability with respect to reinforcement corrosion has been proposed for each DI. These five classes – very low (VL), low (L), medium (M), high (H) and very high (VH) "potential" durability – can be used for example for mixture comparison or quality control. The evaluation of the "potential" durability of a given RC will consist of comparing the values of the measured DIs to the threshold values of the associated classes. Another purpose of this approach is to design concrete mixtures capable of protecting structures against degradation for given target SL and environmental conditions, using performance-based criteria (specifications) related to the DIs. Furthermore, a multi-level modelling concept has been developed for SL prediction [8,14]. It can be applied to predict the SL of a new structure at the design stage or the "residual" lifetime of an existing and possibly deteriorated structure. Since concrete composition, which is often lacking for existing structures, is not needed, this approach can be very easily applied to them, in view of monitoring, diagnosis, maintenance and support to serviceability extension or repair decisions. Note that this is the same DI set, which is involved in the "potential" durability

* Corresponding author. Tel.: +33 1 40 43 51 32; fax: +33 1 40 43 54 98.
*E-mail address:* baroghel@lcpc.fr (V. Baroghel-Bouny).

0958-9465/$ - see front matter © 2011 Elsevier Ltd. All rights reserved.
doi:10.1016/j.cemconcomp.2011.04.007

classes, in the specifications and as input data for the models of SL prediction [7,9,14,15].

Hence, it is important to:

- investigate whether DIs can be assessed by simple and rapid methods, in order to easily include them in a more general set of (sustainability) indicators and in harmonized standard methodologies,
- focus on "green" materials, which incorporate local aggregates or high volumes of supplementary cementitious materials (SCMs) such as fly ash (FA) or ground granulated blast furnace slag (GGBS).

With regard to the second item, it is well known that a complete characterization of SCMs can be very complex [16]. In addition, some properties of one FA for example cannot be generalized to all FAs, since the properties of a given type of SCM can be very variable (e.g. effects of the specific surface area, alkalinity and glass content). However, it is possible to benefit from the numerous researches carried out worldwide over a long period in particular in North America on these materials (see e.g. [17–20]). For example the effect of pozzolanic constituents on pore structure and thus on transport properties has been clearly described in the literature. It is not only a filler effect, but also the result of chemical reactions. The presence of fine particles can also induce acceleration of hydration reactions of the cement (potential nucleation sites for $Ca(OH)_2$ and C–S–H precipitation) and therefore induce earlier densification of the microstructure [21]. These effects are more significant with silica fume (SF), which has a 100-time smaller size than FA. $Ca(OH)_2$ crystals are consumed by the pozzolanic reaction, while finely divided C–S–H hydrate gel is formed, thus yielding a denser microstructure. In addition, when the FA content increases, fibril-type C–S–H are progressively replaced by foil-type C–S–H, which are more efficient to fill capillary pores [22]. Moreover, additional C–S–H (or other gel-type hydrates) form mainly far from the initial cement grains covered by pseudoform C–S–H [23]. These additional C–S–H thus create solid "islands", between partially reacted grains or pre-existing hydrate clusters, which increase the pore network tortuosity. However, this physical effect induced by chemical reactions will be efficient only once the pozzolanic reaction has significantly progressed, which means in the case of FA long after hydration (or pozzolanic reaction with SF [21]) has started (e.g. several months [3,24]). In addition, this effect depends on the initially available $Ca(OH)_2$ amount. Yet, $Ca(OH)_2$ is formed by portland cement hydration and can be affected by early-age drying or carbonation [3,24]. Further, SCMs are known to change the concentration and the mobility of the ions in the pore solution (e.g. as a result of modifications of the electrical double-layer at the solid–liquid interface [23,25–27]). For example, the presence of SF induces a significant decrease in alkali and hydroxyl ion concentrations in the pore solution [28,29], and according to [30] when 30% of the cement is replaced by FA the hydroxyl concentration is also reduced (see also [23]).

This paper will focus on the assessment of DIs, more specifically of the transport properties *effective* chloride diffusion coefficient and "intrinsic" liquid water permeability, by various methods, on a broad range of materials including mortars or concretes with FA, as well as CEM-III concretes. The range of SCM contents has been selected to be relevant from a practical point of view or to be that commonly used in concretes. The purpose is to validate the use of simple and rapid methods (e.g. direct experimental methods or indirect methods based on analytical formulas) and to check their applicability particularly to high-volume SCM mixtures. Comparison with a more theoretical and sophisticated method based on numerical inverse analysis will be carried out in the case of the "intrinsic" liquid water permeability. Another aim is to contribute to the constitution of a database, at least for the concretes most likely to be used in practice, for *apparent*/*effective* chloride diffusion coefficients, "intrinsic" liquid water permeability and electrical resistivity. This will provide in particular an estimate of the values expected for DIs and their corresponding classes, within the framework of the associated performance-based approach. This aspect is very important for future recommendations/standardisation on this topic. Moreover, the specificities of high-volume SCM mixtures will be pointed out.

## 2. Materials and experiments

### 2.1. Materials

A broad range of concretes, ranging from low-grade materials (average 28-day cylinder compressive strength, c.s., approx. 20 MPa) up to very-high-performance concretes (28-day c.s. > 90MPa), has been tested in lab conditions at $T = 21 \pm 1$ °C. Since it is difficult to report in the paper the detailed mix-compositions of all the concretes tested (30), only the mix-composition and the average 28-day cylinder c.s. of the concretes most involved in the discussion and displayed in figures are reported in Table 1. Various CEM I and CEM III (mixtures denoted "-III") were used and the water-to-binder ratio by mass (W/B) ranged from 0.23 to 0.84. The composition of cement #3, which is the CEM I used for the "M" concrete series (see Table 1) and for several other concretes, is given in [31]. With regard to CEM III/A, the GGBS content was 43% (LR59-1-III) or 62% (e.g. BO-III and LR77-3-III) by mass of binder. In order to complement the data, one CEM III/C concrete with 85% GGBS has been tested (denoted B30-III/C [32]). Air-entraining admixture (AEA), FA or SF were incorporated in some of the mixtures (denoted "-EA", "FA" or "SF", respectively). In AEA-mixtures, the air content of the fresh concrete ranged from 2% to 8%. The SF content ranged from 6% to 11% by mass of binder. In the FA-concretes, the FA content was 20% (M25FA, M25FA-EA, M50FA and M50FA-EA [33]), 30% (M30FA), 35% (CFA) or 39% (B50FA) by mass of binder. The same FA was used for the various materials (its composition is given in [31] and its specific surface area is 1.73 $m^2\ g^{-1}$), except for concretes CFA [7] and B50FA. Not only lab mixtures, but also mixtures commonly used in bridges in various locations in France and in neighbouring countries (which include in particular local aggregates) have been studied (e.g. mixtures denoted "LR", such as LR77-3-III which is considered as suitable for exposure class XA2, or LR59-2 for exposure class XS3, according to the European concrete standard EN 206-1 [5]).

Moreover, in order to understand more precisely the FA effect in mixtures of practical interest, mortars with various FA contents (0%, 10%, 20% and 30% by mass of binder = C + FA), denoted FA-0, FA-10, FA-20 and FA-30 respectively, and with limestone filler (60% by mass of binder = C + FA) mainly used to improve the properties of the fresh material, have also been studied. Note that possible synergistic effects between FA and limestone filler are likely to enhance mechanical strength and durability (e.g. acceleration of early hydration, see section 1, formation of carboaluminate by limestone, as well as later strength development and microstructure densification by FA pozzolanicity). The content of binder B = C + FA or of powder materials, as well as W/B, were the same for all the mortars ($B = 511\ kg\ m^{-3}$, W/powder = 0.28, and W/B = 0.45). The same ingredients (cement, FA, and sand) as for the "M" concrete series were used. The amount of admixtures was selected to comply with the proper rheological properties of high-fluidity mortars [34]. FA-30 is regarded in Japan, within the framework of underground disposal facilities (for radioactive wastes) with multicomplex artificial barriers, as a basic mortar

**Table 1**
Mix-composition and average 28-day cylinder c.s. of some of the tested concretes.

| Concrete | CFA | BO-VB | M25 | M30FA | M50 | M75SF | B80SF-S | LR59-1-III | LR77-3-III | BO-III | LR59-2 |
|---|---|---|---|---|---|---|---|---|---|---|---|
| Cement | 1 (CEM I 42.5) | 2 (CEM I 52.5) | 3 (CEM I 52.5) | | | | | 4 (CEM III/A 42.5) | 5 (CEM III/A 52.5) | 6 (CEM III/A 42.5) | 7 (CEM I 52.5) |
| Gravel (G) content (kg m$^{-3}$) | 949 | 1192 | 1007 | 986 | 937 | 1044 | 980 | 980 | 930 | 1036 | 1025 |
| (min/max grain size in mm) | (6/16) | (4/20) | (5/20) | (4/20) | (5/20) | (5/20) | (6/14) | (4/20) | (6.3/20) | (6.3/20) | (4/20) |
| Sand (S) content (kg m$^{-3}$) | 911 | 744 | 899 | 879 | 806 | 877 | 790 | 890 | 800 | 715 | 815 |
| (min/max grain size in mm) | (0/5) | (0/5) | (0/5) | (0/5) | (0/5) | (0/5) | (0/4) | (0/4) | (0/4) | (0/4) | (0/4) |
| Cement (C) content (kg m$^{-3}$) | 260 | 353 | 230 | 223 | 410 | 360 | 420 | 385 | 400 | 342 | 400 |
| Fly ash (FA) content (kg m$^{-3}$) | 140 | | | 95 | | | | | | | |
| Silica fume (SF) content (kg m$^{-3}$) | | | | | | 22 | 35 | | | | |
| Water (W) content (kg m$^{-3}$) | 193 | 172 | 193 | 166 | 197 | 136 | 147 | 159 | 195 | 186 | 150 |
| Plasticizer or superplasticizer content (kg m$^{-3}$) | 4.8 | | | 1.1 | | 12 | 7.28 | 1.14 | 1.2 | | 4.4 |
| Retarder content (kg m$^{-3}$) | | | | 1.4 | | 2.5 | | | | | |
| Water-to-cement ratio (W/C) | 0.74 | 0.49 | 0.84 | 0.74 | 0.48 | 0.38 | 0.35 | | | | 0.38 |
| Water-to-binder ratio (W/B) | 0.48 | 0.49 | 0.84 | 0.52 | 0.48 | 0.36 | 0.32 | 0.41 | 0.49 | 0.54 | 0.38 |
| SCM-to-binder ratio | | | | 0.3 | | 0.06 | 0.08 | 0.43 | 0.62 | 0.62 | 0 |
| Gravel-to-sand ratio (G/S) | 1 | 1.6 | 1.1 | 1.1 | 1.2 | 1.2 | 1.2 | 1.1 | 1.2 | 1.4 | 1.2 |
| Average 28-day cylinder compressive strength (MPa) | 28.9 | 49.5 | 25.1 | 48.5 | 55.5 | 85.5 | 76.9 | 75.5 | 41 | 38.5 | 85.8 |

mixture expected to prevent, for a very long time, diffusion of nuclide molecules emitted from radioactive wastes [34].

### 2.2. Experiments

Electrical resistivity ($\rho'$) measurements, steady-state (ss) and non-steady-state (nss) migration tests, nss diffusion tests, as well as drying experiments, were carried out. The test procedures are detailed in the following sections. In addition, the porosity accessible to water ($\Phi$) was measured by means of hydrostatic weighing [32]. Likewise, mercury intrusion porosimetry (MIP) tests were performed to complement the analysis (assessment of porosity $P_{Hg}$, pore size distribution and critical diameter $d_c$). The test method is described in [32]. The MIP device used allows one to investigate pores with radii from 1.8 nm to 60 μm ($p_{Hg}$max. = 400 MPa), except in some cases, which will be indicated in the paper, where $p_{Hg}$max. = 200 MPa and where the pore radii range consequently from 3.7 nm to 60 μm. "Representative" specimens (several pieces of approx. 1 cm$^3$ each) were prepared for MIP tests by excluding however the coarser pieces of aggregates. Prior to measurement, the specimens were oven dried for 14 days under vacuum at $T = 45 \pm 1$ °C in the presence of silica gel, or freeze-dried [32].

## 3. Electrical resistivity

### 3.1. Significance

Since electrical current is carried mainly *via* the liquid phase (by ions), the pore network connectivity of water saturated hardened cementitious materials can be characterized indirectly by measuring $\rho'$ (inverse of conductivity $\sigma$) [35]. In the general case, $\rho'$ depends not only on porosity and on the tortuosity and connectivity of the pore system, but also on the conductivity of the pore solution ($\sigma_0$), on the surface conductivity of the pore walls (adsorption of elements from the pore solution on C–S–H gel), and on the nature and volume of aggregates.

$\rho'$ can be measured on lab samples. The non-destructive resistivity test can also be used *in situ* for the monitoring of the durability of structures [36]. Some authors have suggested hence that a resistivity test could be used for the control of the production of concretes with pre-defined durability requirements (see e.g. [10,37]). In addition, the *effective* chloride diffusion coefficient could be calculated from a single resistivity measurement (see Section 5.4 and [10,35,38]). Moreover, durability specifications (performance-based criteria) can be based on this parameter [7], and models involving electrical resistivity have also been developed [10,35] for SL prediction, which include both the initiation and propagation periods according to *Tuutti's* definition [39]. $\rho'$ can thus be regarded as an alternate DI [7].

### 3.2. Test method

The technique used here to measure $\rho'$ (Ω m) is described in [40] (see also [10] or [37]). The resistivity test is a simple, quick, cheap and non-destructive method, which however requires some care [41]. It consists in placing a pair of stainless steel electrodes on the parallel surfaces of a sample and measuring the current $I$ (A) induced by the application of a potential drop $\Delta E$ (10 V or less). The electrical contact is ensured by two wet sponges. $\rho'$ is then calculated by geometrical conversion according to *Ohm's* law (see Eq. (1)):

$$\rho' = \frac{\Delta E}{I} \cdot \frac{A}{e} \quad (1)$$

where $A$ (m$^2$) is the cross sectional area of the electrodes (*i.e.* of the sample) and $e$ (m) is the distance between electrodes (*i.e.* the height of the sample).

Literature indicates that the reproducibility coefficient of variation (COV) is 9–30% (see e.g. [36,42,43]) and the repeatability COV is 11% [42].

### 3.3. Results and discussion

$\rho'$ was measured on a broad range of water-cured and water-saturated materials at various ages. Fig. 1 displays the concrete results (average values of three samples) plotted *vs.* the average 28-day cylinder c.s. The classes of "potential" durability with respect to reinforcement corrosion (VL, L, M and H, see Section 1) are also reported in the graph (the associated thresholds are 50, 100, 250 and 1000 Ω m [7]). Fig. 2 displays the experimental results obtained for the mortars.

Fig. 1 shows that the presence of FA, GGBS or SF induces high resistivity values. For example, HPCs with SF display values between 380 and 670 Ω m, thus indicating a high "potential" durability. This results from the various effects of SCM on the pore structure (see Section 1). In addition, as detailed in section 1, the

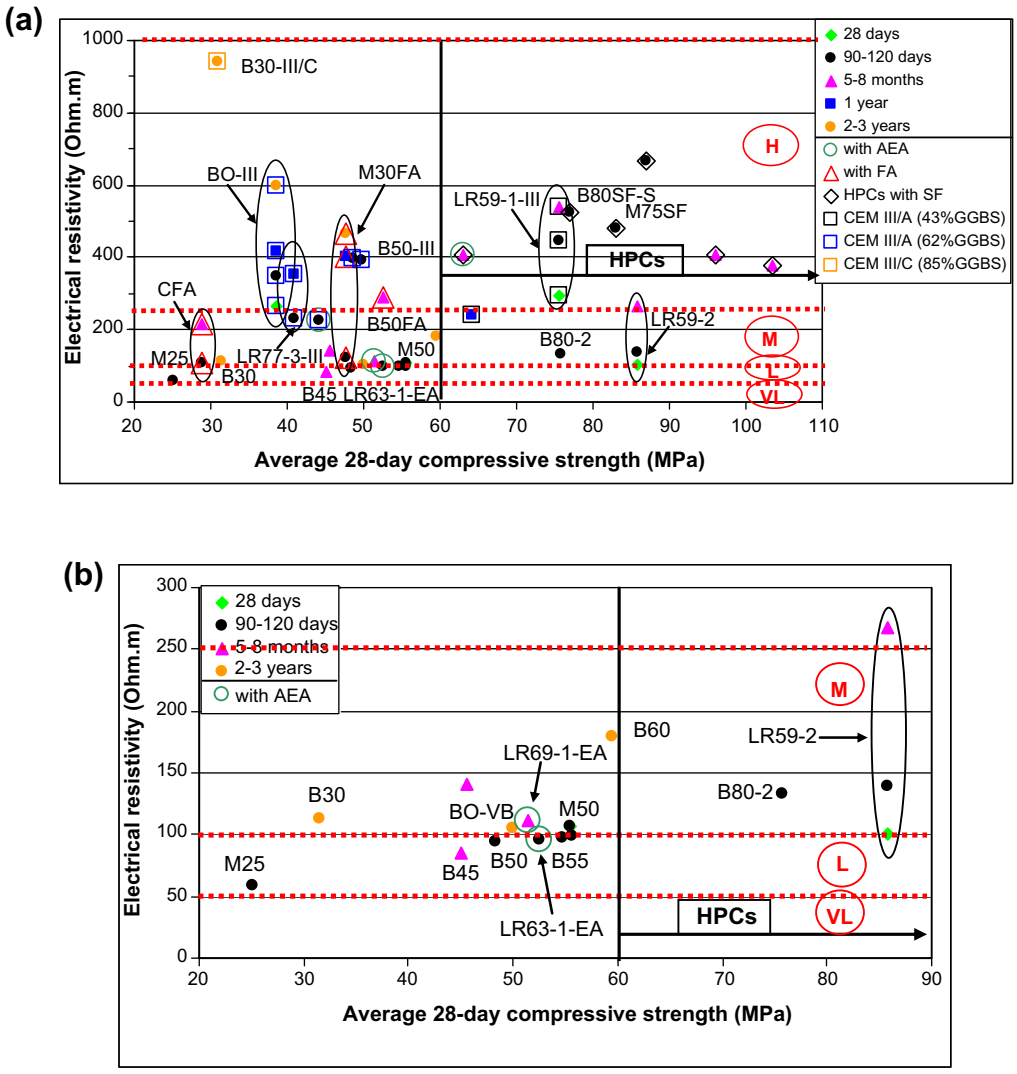


**Fig. 1.** "Potential" durability classes (H, M, L, and VL) and experimental mean values of electrical resistivity measured on various water-cured and water-saturated concrete samples *vs.* the average 28-day cylinder c.s. *Circled data: same mixture and various ages.* (a) Complete range of concretes tested. (b) Plain OPC – CEM I concretes (zoom).

presence of SF induces a significant decrease in the alkali and hydroxyl ion concentrations in the pore solution. Since the conductivity of the pore solution $\sigma_0$ can be estimated from the major contribution of $Na^+$, $K^+$ and $OH^-$, $\sigma_0$ will decrease and so also the conductivity of the porous material $\sigma$ ($\sigma$ is proportional to $\sigma_0$ [44]). This will induce an increase in $\rho'$. However, Fig. 3a, which displays MIP results (see Section 2.2) obtained on HPCs B80-2 and B80SF-S, confirms that the marked difference recorded on $\rho'$ between HPCs with and without SF, for the same c.s. and age (see Fig. 1), here ≈76 MPa and 90 days (and even for a similar MIP porosity, here ≈7.5%, see Fig. 3a), results mainly from the drastic refinement of the pore structure. Concretes with a high FA content (between 30% and 39% by mass of binder) display $\rho'$ values between 110 and 465 Ω m, while CEM III/A concretes (with 43 or 62% GGBS by mass of binder) display values between 230 and 595 Ω m, depending on the age (medium or high "potential" durability). In the case of CEM III/C with 85% GGBS (B30-III/C), the value recorded at the age of 3 years reaches 945 Ω m (high "potential" durability). For each binder type (0–10%, 20% and 30% FA) and for given constituents, a rather linear relationship is pointed out between $\rho'$ and c.s. measured at the same age (see Fig. 2b). In addition, at a given c.s., when the FA content increases, there is a shift towards higher $\rho'$ values (see Fig. 2b).

In Fig. 1 the circled values denote the results obtained for the same concrete at various ages (e.g. BO-III: 28 days, 90 days, 1 year and 2 years) and point out the significant $\rho'$ increase with the age for FA- or CEM-III/A-concretes. Likewise, Fig. 2a shows the increase in the mortar resistivity with age (and FA content). This results from the microstructural changes induced by hydration and pozzolanic reactions (see Section 1). This increase is well correlated with the evolution of the MIP pore size distribution (see Fig. 4 and [3,24,34] for FA-materials). The resistivity of plain OPC – CEM I materials also increases with age but to a lesser extent (see Fig. 1), as already reported in the literature (see e.g. [45]).

As illustrated in Fig. 2a, when the pozzolanic reaction with fly ash has not progressed very much (age = 90 days), the $\rho'$ values are very similar in the case of 0, 10, 20 and 30% FA. In particular, the difference between FA-0 and FA-10 becomes significant only at 180 days. The (slight) difference, which is recorded between the cases 20–30% FA and 0–10% FA at 90 days, could be explained by the decrease in the connectivity induced by the filler effect associated with the presence of 20–30% FA, a slight pozzolanic effect, the acceleration of hydration and therefore of the densification of the microstructure, or the decrease in the concentration of some ions in the pore solution in the presence of FA (see Section 1). Nevertheless, the similarity of the $\rho'$ values at 90 days for the various

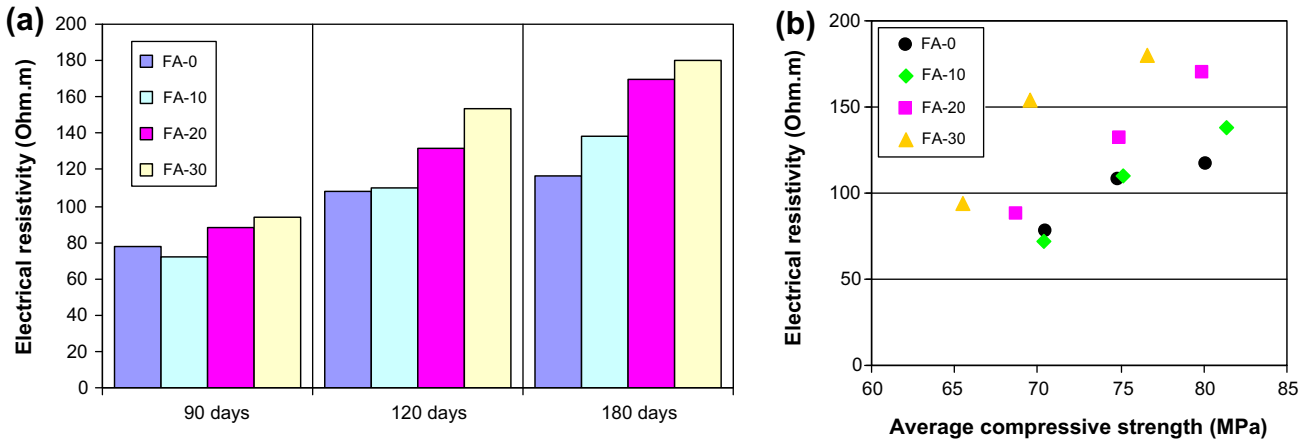


**Fig. 2.** Experimental mean values of electrical resistivity measured on water-cured and water-saturated mortar samples (W/B = 0.45) with various FA contents (0, 10, 20 and 30% by mass of binder). (a) At various ages. (b) As a function of the cylinder c.s. at the same age.

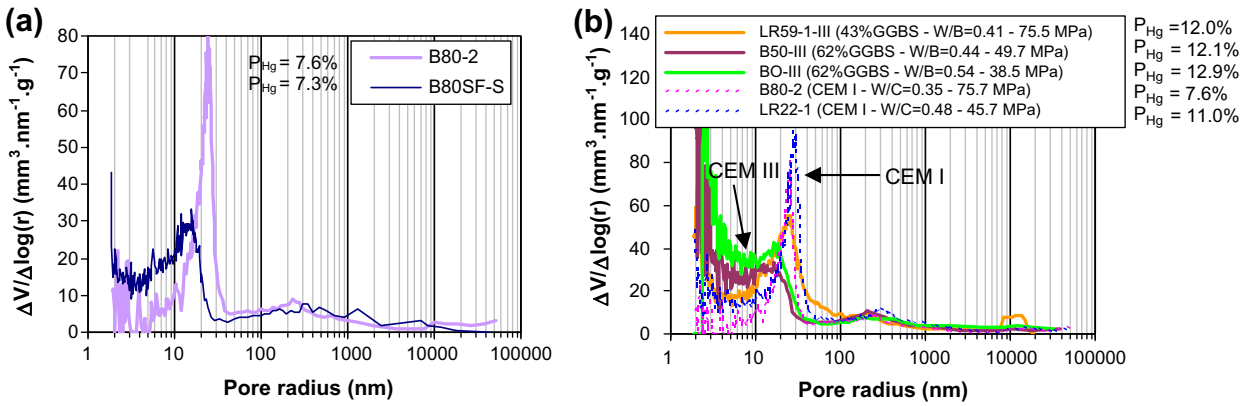


**Fig. 3.** MIP pore size distributions measured in concrete samples at 90 days after water curing and 14-day oven drying at $T = 45 \pm 1$ °C under vacuum and with silica gel. *The porosity values $P_{Hg}$ are also reported.* (a) Concretes B80-2 (SF/C = 0) and B80SF-S (SF/C = 0.08) prepared with W/C = 0.35 and cement #3. (b) Comparison between CEM III/A and CEM I concretes.

FA contents indicates that this last effect does not significantly affect the measurement. Therefore, comparison between materials with and without FA by using the resistivity parameter is quite valid and the difference recorded at later ages can mainly be explained by changes in the pore structure (refinement). These findings tend to confirm that electrical resistivity is a good indicator of the connectivity of the pore network for both OPC and FA materials. Nevertheless, the analysis is easy in the case of the mortars studied here, since the various mixtures have the same constituents.

With regard to plain OPC – CEM I mixtures with 28-day c.s. ranging from 25 MPa (M25, W/C = 0.84, see Table 1) to 86 MPa (LR59-2, W/C = 0.38, see Table 1), the $\rho'$ values range from 60 to 200 Ω m between 28 days and 1 year, therefore displaying low or medium "potential" durability (see Fig. 1). These values are in agreement with the data reported in the literature (e.g. 50–200 Ω m in [36]).

For any given type of binder (e.g. CEM I, CEM I + SF, CEM I + FA or CEM III/A), electrical resistivity does not depend very much on the 28-day c.s. (in particular on the W/B): the range of $\rho'$ values measured is small even if the range of 28-day c.s. is very large, compared to the variation induced on the $\rho'$ value when changing the binder type at a given 28-day c.s. (see Fig. 1). Therefore, for example in the case of plain OPC – CEM I mixtures, within a broad 28-day c.s. range, resistivity measurement does not seem very discriminating, in particular when the data are compared to values obtained with FA-, GGBS- or SF-concretes (see Fig. 1). This may be problematic in practical situations. This observation can be explained first by the fact that the pore system connectivity is more drastically changed by including SCM than by keeping CEM I and changing W/C (e.g. between 0.35 and 0.50). Likewise, changing W/B (e.g. 0.44 and 0.54) of 62%-GGBS CEM III/A concretes does not significantly change the pore system. All of this is clearly illustrated by the MIP pore size distributions displayed in Fig. 3b. In addition, for plain OPC – CEM I materials, when W/C increases significantly (in particular for W/C $\geqslant$ 0.50), ionic concentrations decrease significantly in the pore solution and consequently $\sigma_0$ decreases [46,47]. This will induce an increase in $\rho'$, which counteracts the decrease induced by the higher pore network connectivity. Note that the (overall) $\rho'$ value measured in this case does not reflect only the connectivity of the pore system and cannot be rigorously directly compared to the values obtained for other materials.

According to the results presented in Fig. 1, no systematic effect of AEA is observed on $\rho'$.

It can be concluded from all of these observations that electrical resistivity measurement is, in the general case and in particular in the case of high-volume SCM mixtures, an easy method to characterize the connectivity of the pore system. However, the ionic composition of the pore solution (which depends on the composition of binder and aggregates, and of W/C) can significantly affect the overall $\rho'$ value measured in the case of high-porosity plain

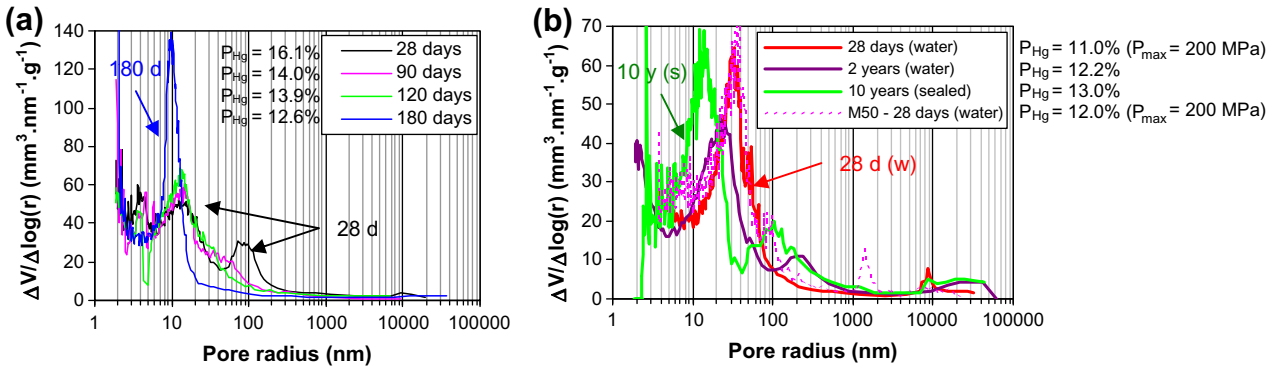


**Fig. 4.** MIP pore size distributions of 30%-FA materials after various curing conditions in lab. *The porosity values $P_{Hg}$ are also reported.* (a) Mortar FA-30 after 28-, 90-, 120- and 180-day water curing in lab (and freeze drying). (b) Concrete M30FA after 28-day and 2-year water curing and after 10-year sealed curing in lab (and 14-day oven drying at $T = 45 \pm 1$ °C under vacuum and with silica gel). Comparison with M50 at 28 days.

OPC – CEM I concretes (see also [40]). As a consequence, electrical resistivity will be more appropriate to distinguish the binder type, in particular the presence and the amount of SCM compared to plain OPC – CEM I concretes, than to distinguish (and rank) various CEM I (or CEM III/A) concretes. It seems hence difficult to provide a single ranking based on resistivity for a wide range of concretes.

## 4. Apparent chloride diffusion coefficient

### 4.1. Significance and direct assessment from non-steady-state migration test

The *apparent* chloride diffusion coefficient is the global coefficient involved in *Fick's* second law, which takes into account binding. It is used for example as input data in empirical models of chloride ingress [6,7].

The colorimetric measurement ($AgNO_3$ spray test) of the average chloride penetration depth ($x_d$), after a nss migration test under an external electrical field, allows, with several assumptions [48], the easy and rapid assessment of an *apparent* chloride diffusion coefficient $D_{ns(mig)}$ by applying the modified *Nernst–Planck* equation. As a matter of fact, in saturated conditions, the advection flow term of this equation can be neglected. In addition, when both the electrical field $\Delta E/e$ and $x_d$ are large enough ($x_d > (\Delta E/e)\cdot(ZF/RT)\cdot D_{ns(mig)}\cdot t$), the diffusion term of the equation can also be neglected with respect to the electrical migration term [49]. Moreover, activity effects and interactions between ions can be neglected by assuming very dilute solutions and chlorides as the single species in the pore solution, respectively. Hence, $D_{ns(mig)}$ can be calculated by the following widely used solution proposed by Tang and Nilsson [50] (see Eq. (2)):

$$D_{ns(mig)} = \frac{R \cdot T}{Z \cdot F'} \cdot \frac{e}{\Delta E} \cdot \frac{x_d - \alpha \cdot \sqrt{x_d}}{t} \quad (2)$$

where $t$ denotes the test duration (s), $e$ the sample thickness (m), $Z$ the valence number of chloride ion ($Z = 1$), $F'$ the Faraday constant ($F' = 96{,}480$ J V$^{-1}$ mol$^{-1}$), $\Delta E$ the actual electrical potential drop between the two sides of the sample ($V$), $R$ the ideal gas constant ($R = 8.3144$ J mol$^{-1}$ K$^{-1}$), and $T$ the absolute temperature (K). $\alpha$ is the auxiliary term defined in [50] as a function of the test conditions.

A test based on this principle has been standardized in the Nordic countries [51]. The COV of this test is reported to be max. 24% (resp. 15%) with regard to reproducibility (resp. repeatability) for all types of concretes according to [42] and [51].

Here, nss migration tests have been carried out after vacuum saturation of the samples ($e = 50 \pm 1$ mm; diam. = 110 mm) with a 0.1 M NaOH solution. For these tests, the samples were epoxy-coated around their cylindrical surface and mounted between the two compartments of a so-called migration cell [48,52]. The cell-sample interface was also coated with epoxy, in order to insure a watertight joint. The upstream compartment (catholyte) contained (0.5- or 1-M) NaCl + 0.1-M NaOH, while the initial downstream solution (anolyte) was 0.1-M NaOH. The volume of each compartment solution was 1 l. An external potential drop was applied by electrodes at the sample boundaries and kept constant during the test. Its value has been restricted to max. 30 V. Depending on the mix-composition and on the potential drop value, the test lasted between 1 day and a few days. It has been checked that the test conditions were appropriate for the computation of $D_{ns(mig)}$ (shape of the experimental profiles close to the theoretical one, confirming negligible diffusion, ..., see above and [48]).

### 4.2. Results and discussion

The *apparent* chloride diffusion coefficient $D_{ns(mig)}$ (average values of three samples) measured according to the method described in Section 4.1 on a large number of concretes after water curing and vacuum saturation is plotted *vs.* the average 28-day cylinder c.s. of the materials in Fig. 5. The L, M, H and VH classes, as previously defined, are reported in the graph (associated thresholds: 50, 10, 5 and $1 \times 10^{-12}$ m$^2$ s$^{-1}$, respectively [7]). The results obtained on the water-cured mortar samples are presented in Fig. 6.

It is worth noting that for plain OPC – CEM I mixtures (with local aggregates) currently used in common bridges in various areas in France, the $D_{ns(mig)}$ values (28 days–1 year) are $6–17 \times 10^{-12}$ m$^2$ s$^{-1}$. For these mixtures, a medium or low "potential" durability is therefore obtained (see Fig. 5).

The values circled in Fig. 5 show the decrease in $D_{ns(mig)}$ when age increases for a given concrete. Likewise, Fig. 6 shows the decrease in $D_{ns(mig)}$ when age increases in the case of the mortars. The decrease in $D_{ns(mig)}$ even after 1 year has been reported in the literature in the case of high-volume FA mortars with similar W/B as tested here [53].

Fig. 5 clearly illustrates, for the same average 28-day c.s., the efficiency of SF, FA or GGBS in reducing the *apparent* chloride diffusion coefficient: a higher durability level (class) is reached with SCM materials, compared to plain OPC – CEM I mixtures with the same average 28-day c.s. For example, the presence of SF induces a shift from the H to VH class. Furthermore, a good consistence is obtained from a given age between the values measured, on the one hand, on the various CEM-III concretes and, on the other hand, on the various FA-concretes tested. With regard to $D_{ns(mig)}$, the effect of SCM is more significant than that of W/B. For example,

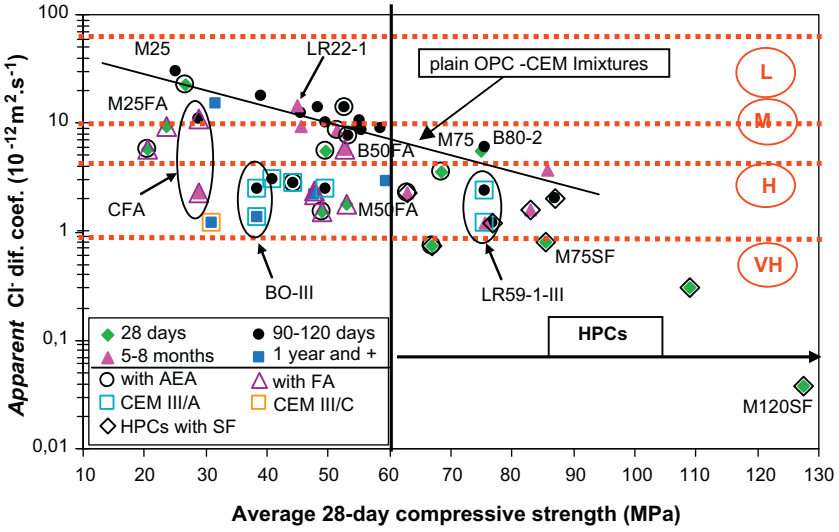


**Fig. 5.** "Potential" durability classes (VH, H, M, and L) and experimental mean values of *apparent* chloride diffusion coefficient $D_{ns(mig)}$ measured by nss migration test under an external electrical field on saturated water-cured concrete samples at various ages *vs.* the average 28-day cylinder c.s. *Circled data: same mixture and various ages.*

CEM III/A concretes with 28-day c.s. ranging from 40 to 75 MPa (*i.e.* W/B from 0.44 to 0.54) exhibit $D_{ns(mig)} = 2.4–3 \times 10^{-12}$ m$^2$ s$^{-1}$, and thus very similar coefficients within this W/B range. In addition, the values recorded for FA- and GGBS-concretes are in this case very close to those found for HPCs (see Fig. 5). In other words, the effect of W/B on $D_{ns(mig)}$ can be significantly mitigated in the presence of FA or GGBS.

Normal-strength FA concretes (from 20% to 35% FA by mass of binder) display very low coefficients and a high "potential" durability. More precisely, concretes with 28-day c.s. approx. 50 MPa, with the same cement and 20–30% FA exhibit $D_{ns(mig)} = 1.5–2.4 \times 10^{-12}$ m$^2$ s$^{-1}$ between 28 days and 1 year (see Fig. 5). The efficiency of FA to decrease $D_{ns(mig)}$ is also illustrated for the mortars in Fig. 6. The reduction in the chloride diffusion coefficient in saturated conditions, with the increase in the FA content, illustrated in Fig. 6, has also been widely reported in the literature for lab data [23,25,30,54,55] and also for field data [11,56–58], despite a porosity often higher in particular at early age (dilution effect) (see [34] for the mortars studied here). These findings result from the refinement of the pore structure (as previously explained, see Sections 1 and 3.3). They also result from different chemical and physical chloride–matrix interactions (e.g. electrical double layer, see Section 1), as well as from different electrical interactions between ions in the pore solution, since the *apparent* chloride diffusion coefficient is affected by these interactions. For example, physical interactions vary with the pore solution composition. And according to the literature [23,55], the nature and quantity of cations in FA-materials increase the resistance to diffusion of chloride anions: the higher calcium, silicon and aluminate concentrations and the lower potassium concentration decrease chloride mobility. Nevertheless, as shown in Fig. 6a, the efficiency of FA in realistic mixtures is more marked after 180 days than after 90 days. The same conclusion can be made when comparing the results for CFA (35% FA) at 4 and 7 months (see Fig. 5). Furthermore, as illustrated by the B50FA result in Fig. 5, 180 days can still be too early to observe the beneficial effect of the high FA amount (39%) (as it takes time to develop a significant amount of additional C–S–H) to exceed its detrimental effect (coarse, porous and heterogeneous initial microstructure [59]) (see also [53,60]). This is further pointed out when comparing B50FA to

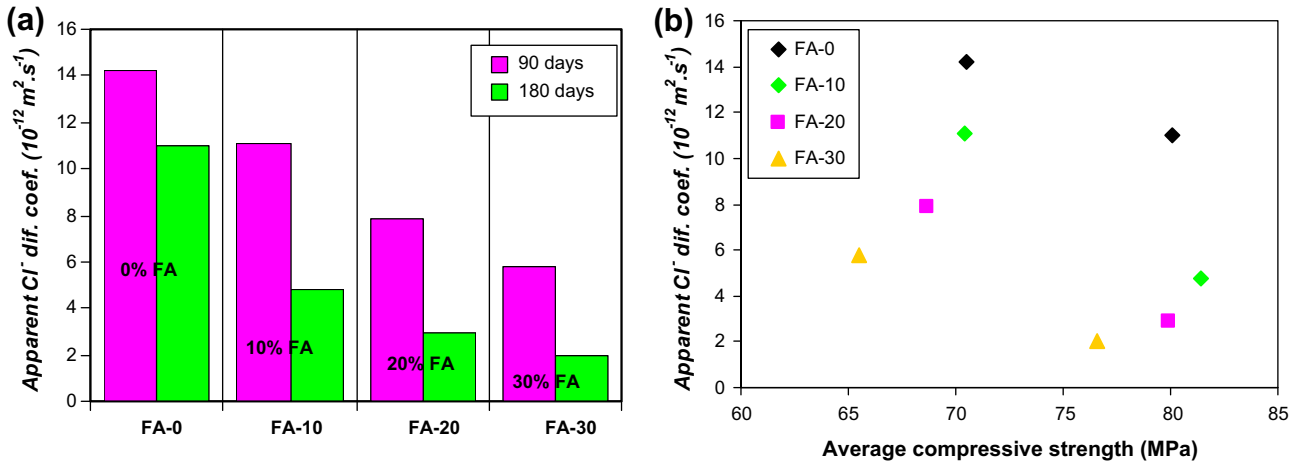


**Fig. 6.** Effect of the FA content on the *apparent* chloride diffusion coefficient $D_{ns(mig)}$ measured by nss migration test under an external electrical field on the saturated mortar samples (W/B = 0.45), after 90-day or 180-day water curing. (a) At various ages. (b) As a function of the cylinder c.s. at the same age.

M50FA (20% FA) (see Fig. 5). Therefore, above 30% cement replacement, the time required to record a significant beneficial FA effect on $D_{ns(mig)}$ seems long. This is consistent with the optimum value (30%) found in the literature at medium term [61] and with the values currently used in practice.

CEM III/A or CEM III/C concretes display a high "potential" durability. This is in agreement with the literature, where it is reported that the chloride diffusion rate in GGBS concretes is much lower than in CEM-I materials and even than in 30%-FA materials, mainly as a result of the high tortuosity of the pore system and of matrix–chloride interactions (see Section 3.3 and e.g. [62–65]).

No systematic effect of the presence of AEA is recorded on the *apparent* chloride diffusion coefficient, since diffusion (in saturated conditions) is limited by the smallest pores, even if a (discontinuous) macropore network exists.

Since $D_{ns(mig)}$ decreases as a function of the age and reaches very low values in GGBS- or FA-materials, the value for aged materials is in this case more difficult to determine accurately according to the resolution limit of the method (*i.e.* clear and precise detection of $x_d$), and this is enforced by the dark colour of high-volume GGBS materials [48]. Therefore, the evolution of $D_{ns(mig)}$ as a function of the age in the medium or long term can be more difficult to quantify than that of the electrical resistivity ($\rho'$ increases as a function of the age).

Finally, Fig. 5 shows that a large range of $D_{ns(mig)}$ values and different "potential" durabilities can be obtained for the same average 28-day c.s. (or W/B), depending on the mix-composition. This is a clear illustration of the consequences of the new trends of concrete mix-design and of the relevance and the usefulness of a performance-based approach for durability assessment of complex mixtures. The 28-day c.s. (and thus W/B), which is often regarded as an implicit DI in particular in current standards and recommendations, is not sufficient to estimate the "potential" durability of a RC and to select the appropriate mixture that meets durability requirements. Only a performance approach based on a set of DIs can in particular account for the gain provided by SCMs (and further by a combination of SCMs) for a given 28-day c.s.

## 5. Effective chloride diffusion coefficient

### 5.1. Significance and methods of assessment

The *effective* chloride diffusion coefficient, which is the pure transport property (no binding effect) involved in *Fick's* first law or in the *Nernst–Planck* equation, is an important parameter. It is required, for example, as input data for predictive physical models of chloride ingress and more generally of ion transport [3,7,14,66,67]. This is an "intrinsic" material property, not dependent of the chloride concentration [65,67]. It can be measured in saturated conditions directly by means of a ss migration test. It could also be assessed by simple analytical formulas from parameters already measured in this paper: the electrical resistivity (see Section 3.3) or the *apparent* chloride diffusion coefficient (see Section 4.2), which both involve an easier and quicker test, compared to the ss migration test.

### 5.2. Direct assessment of the effective chloride diffusion coefficient $D_{ss(mig)}$ from steady-state migration test

An *effective* chloride diffusion coefficient $D_{ss(mig)}$ can directly be assessed by means of a ss migration test from monitoring by potentiometric titration the chloride ion concentration *vs*. time in the downstream compartment of the migration cell where the concrete or mortar sample is tested. When the chloride flux and the potential drop at the boundaries of the sample are constant, $D_{ss(mig)}$ is provided by the modified *Nernst–Planck* equation, where the diffusion and advection flows are neglected with respect to the electrical migration one, and with the assumption of very dilute solutions and no interaction between ions in the pore solution (see Eq. (3)) [68,69]:

$$D_{ss(mig)} = \frac{R \cdot T}{Z \cdot F'} \cdot \frac{e}{\Delta E} \cdot \frac{Q}{\gamma \cdot c_0 \cdot t} \tag{3}$$

where the chloride concentration of the catholyte solution (upstream compartment) $c_0$ (mol/m$^3$ of solution) is assumed to be a constant, $\gamma$ is the activity coefficient of chloride ion in the catholyte solution (–) and $Q$ denotes the cumulative amount of chloride ions arriving in the downstream compartment during time $t$ within the ss regime.

The constant chloride flux $Q/t$ within the ss regime, required for the calculation of $D_{ss(mig)}$, is assessed from the slope of the linear part of the plot giving the cumulative chloride amount *vs.* time.

Note that two other techniques can be used to assess $D_{ss(mig)}$ from a ss migration test: conductivity measurement in the downstream compartment [70] or titration in the upstream compartment [71]. It was shown that the three techniques yield similar $D_{ss(mig)}$ results (see [3,8,72]). Nevertheless, it is worth noting that $D_{ss(mig)}$ measurement can suffer from poor accuracy in some cases as far as reproducibility is concerned: the COV was found equal to 76% with regard to reproducibility in the case of a conductivity measurement, according to [42]. The value of 22% is reported in the same reference for the repeatability COV.

Ss migration tests have been carried out here on 20-mm thick samples, according to [72], by using similar cells as those described for nss migration tests (see Section 4.1). Here, the upstream solution was 1-M NaCl + 0.1-M NaOH, while the initial downstream solution was 0.1-M NaOH. The actual potential drop between the surfaces of the sample was measured during the test by means of two reference electrodes contacting the sample surfaces.

Fig. 7 displays the *effective* chloride diffusion coefficients $D_{ss(mig)}$ (average values of three samples) directly assessed from ss migration tests by potentiometric titration in the downstream compartment *vs*. the average 28-day cylinder c.s. The classes of "potential" durability L, M, H and VH, as previously defined, are also reported in the graph (associated thresholds between classes: 8, 2, 1 and $0.1 \times 10^{-12}$ m$^2$ s$^{-1}$, respectively [7]). Similar observations can be made as in the case of $D_{ns(mig)}$. Again, normal-strength FA-mixtures (20–35% FA) or GGBS-mixtures (62% GGBS) are shown to be out of the range obtained with plain OPC – CEM I materials (significantly lower $D_{ss(mig)}$ values are obtained). On the other hand, no deviation is recorded in the case of B50FA (39% FA and age = 4 months) (see Section 4.2) and a slight deviation is recorded in the case of LR59-1-III (43% GGBS and age = 8 months), compared to plain OPC – CEM I materials. These are typically cases where incorporation of another SCM (*i.e.* ternary blends) can be beneficial for both short-term and long-term durability. For example, as previously mentioned 4 months is too early to reveal the significant (but delayed) beneficial effect of 39% FA. SF incorporation in this case would allow a decrease of $D_{ss(mig)}$ even in the short and medium terms.

### 5.3. Assessment of the effective chloride diffusion coefficient from non-steady-state diffusion test ($D_{eff(dif)}$) or from non-steady-state migration test ($D_{eff(mig)}$)

In the case of diffusion and with some assumptions, the *effective* and *apparent* coefficients, $D_{eff(dif)}$ and $D_{ns(dif)}$ respectively, where $D_{ns(dif)}$ is directly measured by a nss diffusion test [48,52,72], are linked by the following Eq. (4):

$$D_{eff(dif)} = \Phi \cdot (1 + k_d) \cdot D_{ns(dif)} \tag{4}$$

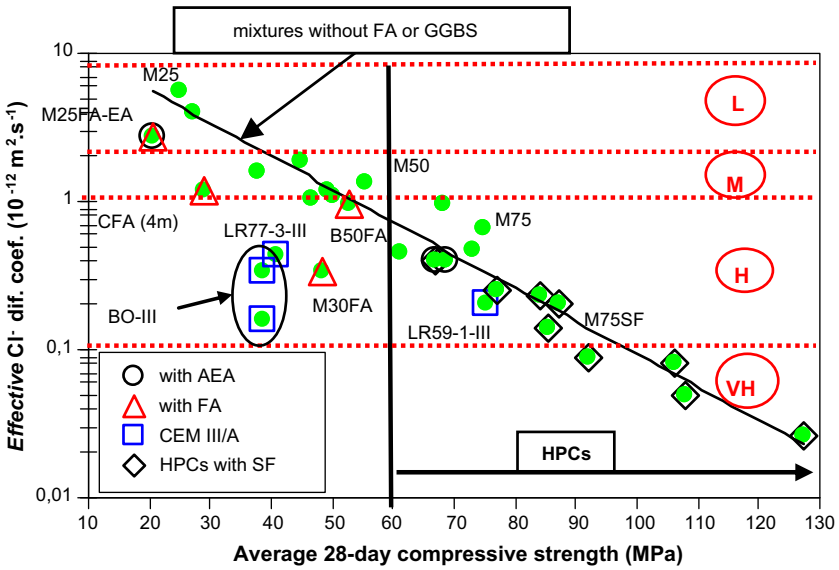


**Fig. 7.** "Potential" durability classes (VH, H, M, and L) and experimental mean values of *effective* chloride diffusion coefficient $D_{ss(mig)}$ measured by ss migration test under an external electrical field on saturated concrete samples (90-day to 1-year water curing) *vs.* the average 28-day cylinder c.s. *Circled data: same mixture and various ages.*

where the so-called chloride binding capacity $k_d$ (expressed here in mass by mass) is the average slope of the binding isotherm (or the slope of the isotherm assumed as linear) within the chloride concentration range considered.

*Tang* demonstrated that a similar linear relationship could be written for migration tests, which involves the *apparent* coefficient $D_{ns(mig)}$ measured by the nss migration test according to [51] and the *effective* diffusion coefficient $D_{eff(mig)}$ [49,73]. Moreover, authors often assume that chloride binding can be neglected [66,67] or is at least reduced [73] during nss migration tests. As a matter of fact, during these tests the velocity of the ions transported through the pore structure is very high and the contact time is short (usual test duration: 10–60 h). Therefore, a non-equilibrium state is expected and the hypothesis of instantaneous binding is not valid, as demonstrated in [74]. A very weak binding is expected (adsorption and maybe chemical reactions are impeded), compared to diffusion where equilibrium binding takes place, and binding may even be suppressed (in particular in the case of low-aluminate content materials). *Castellote* et al. [75] did point out a weak interaction in this kind of test, through fitting the experimental binding isotherm to a general BET equation (by assuming yet local equilibrium). Likewise, *Baroghel-Bouny* [3] obtained significantly weaker binding on BO-VB and M25, compared to the case of nss diffusion, by measuring chloride concentration profiles as soon as possible after the tests. Therefore, as a first approximation, the *effective* chloride diffusion coefficient $D_{eff(mig)}$ can be deduced from the *apparent* chloride diffusion coefficient $D_{ns(mig)}$ directly assessed by means of a nss migration test (in the conditions described in Section 4.1) and by assuming no binding ($k_d = 0$). In this case, $D_{eff(mig)}$ is calculated by Eq. (5):

$$D_{eff(mig)} = D_{ns(mig)} \cdot \Phi \tag{5}$$

### 5.4. Assessment of the effective chloride diffusion coefficient $D_{eff(resistivity)}$ from electrical resistivity measurement

An *effective* chloride diffusion coefficient $D_{eff(resistivity)}$ can theoretically be calculated from an electrical resistivity measurement, by using the modified *Nernst–Einstein* equation (a particular case of the *Nernst–Planck* equation using electrolyte equivalent conductivity as the main parameter [68,76], see Eq. (6)), which can be derived in Eq. (7):

$$\frac{\sigma_0}{\sigma} = \frac{D_0}{D_{eff}} = F \tag{6}$$

$$D_{eff(resistivity)} = \frac{D_0}{\sigma_0} \cdot \frac{1}{\rho'} = \frac{B}{\rho'} \tag{7}$$

where $F$ is the so-called formation factor, $D_0$ is the free diffusion coefficient of chlorides in the pore solution, and $D_{eff}$ denotes the *effective* chloride diffusion coefficient in the porous material.

The *effective* chloride diffusion coefficient is thus inversely proportional to the electrical resistivity $\rho'$ of the water-saturated material and the coefficient B is dependent of the ionic concentrations (of the pore solution).

In order to assess $D_{eff(resistivity)}$ from resistivity measurement, $\sigma_0$ should be determined for each material considered. $\sigma_0$ can be directly measured after pore solution expression [28]. Nevertheless, this requires specialized equipment and the very small volume then extracted could induce errors in the determination of $\sigma_0$. In addition, the measurement can be practically impossible for mature concretes with low W/B. Hence, as a first approximation, the value $\sigma_0 = 11.87\ \Omega^{-1}\ m^{-1}$ currently assumed for alkaline solutions similar to pore solutions of cementitious materials will be adopted here [77]. Likewise, the value $D_0 = 1.484 \times 10^{-9}\ m^{-2}\ s^{-1}$ reported in the literature for the free diffusion coefficient of chloride ions in a 1-M solution at 25 °C [44,78] will be adopted here. By assuming these values, Eq. (8) is derived:

$$D_{eff(resistivity)} \approx \frac{125}{\rho'} \quad (\text{in } 10^{-12}\ m^2\ s^{-1}, \text{when } \rho' \text{ is in } \Omega\ m) \tag{8}$$

Note that Eq. (8) is quite similar to the formula proposed by *Andrade* et al. for 1-M NaCl external solutions [10].

However, according to the comments given in Section 3.3, $\sigma_0$ will significantly decrease in the case of plain OPC – CEM I concretes when W/C is high (typically W/C $\geqslant$ 0.50). Therefore, Eq. (8), which has been obtained with a usual $\sigma_0$ value, will not be valid and $\sigma_0$ needs to be recalculated in this case. This can be done theoretically by means of Eq. (9), by assuming very dilute solutions ($\gamma_i = 1$), no relative diffusion and no interaction between ions in the solution [79,80]:

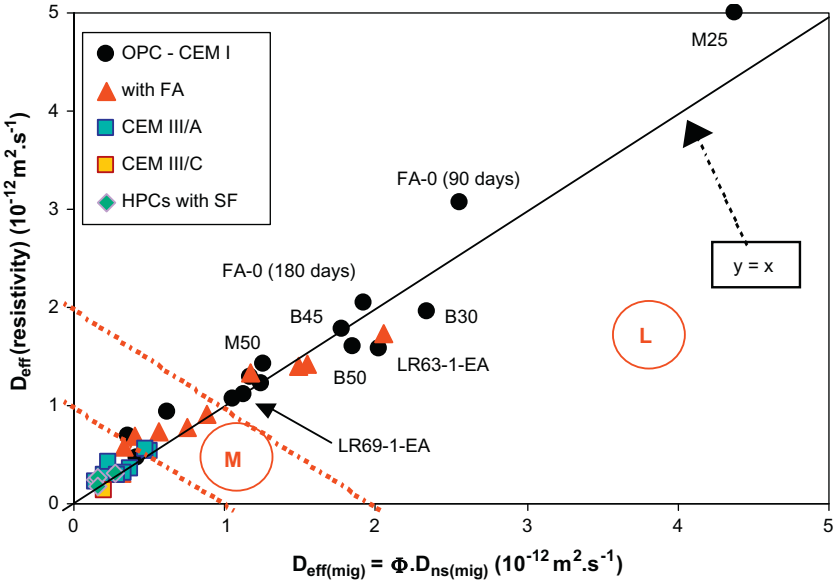


**Fig. 8.** Comparison between the *effective* chloride diffusion coefficients obtained from nss migration tests and from electrical resistivity, on saturated samples of various water-cured concretes and mortars. *The "potential" durability classes (M and L) are also indicated.*

$$\sigma_0 = \frac{F'^2}{R \cdot T} \cdot \sum_i D_i \cdot Z_i^2 \cdot c_i \quad (9)$$

where $\gamma_i$, $D_i$, $Z_i$ and $c_i$ are the activity coefficient (–), the *effective* diffusion coefficient ($m^2$ $s^{-1}$), the valence number (–), and the concentration (mol/$m^3$ of solution) respectively, associated with each ion i.

As mentioned in Section 3.3, $\sigma_0$ can be estimated from the major contribution of the ions $Na^+$, $K^+$ and $OH^-$. $c_{Na+}$ and $c_{K+}$ will be computed from the cement composition (assuming a total alkali release) and $c_{OH-}$ will be deduced from the electroneutrality condition [67]. The computation has been performed for M25 and M50 (W/C = 0.84 and W/C = 0.48 respectively, see Table 1), as well as for a concrete (M40) prepared with the same constituents but with an intermediate W/C (W/C = 0.62). The following $\sigma_0$ values were then obtained: 5.0 $\Omega^{-1}$ $m^{-1}$ (M25), 6.7 $\Omega^{-1}$ $m^{-1}$ (M40), and 9.8 $\Omega^{-1}$ $m^{-1}$ (M50). These computed values were verified by direct measurement on synthetic pore solutions $\sigma_0$ for each tested concrete, classes can be defined around these values and formulas can be proposed for $D_{eff(resistivity)}$ within these classes, for plain OPC – CEM I concretes (or FA concretes when FA have not reacted) (see Eqs. (10)-(12), where $D_{eff(resistivity)}$ is in $10^{-12}$ $m^2$ $s^{-1}$ when $\rho'$ is in $\Omega$ m):

$$\text{For W/C} = 0.45 - 0.55 \quad \sigma_0 = 9.8\ \Omega^{-1}\ m^{-1} \text{ and } D_{eff(resistivity)} \approx \frac{151}{\rho'} \quad (10)$$

$$\text{For W/C} = 0.60 - 0.70 \quad \sigma_0 = 6.7\ \Omega^{-1}\ m^{-1} \text{ and } D_{eff(resistivity)} \approx \frac{221}{\rho'} \quad (11)$$

$$\text{For W/C} \geqslant 0.80 \quad \sigma_0 = 5.0\ \Omega^{-1}\ m^{-1} \text{ and } D_{eff(resistivity)} \approx \frac{297}{\rho'} \quad (12)$$

The proposed Eqs. (10) to (12) allow one to extend the application of the very simple "resistivity method" to high-W/C plain OPC – CEM I concretes.

### 5.5. Comparison of methods – results and discussion

The simple methods proposed from $D_{ns(mig)}$ (see Eq. (5)) or from resistivity measurement, described in the previous sections, are compared in Fig. 8. In order to investigate further the validity of these simple (but indirect) methods, the associated results have been compared to the *effective* chloride diffusion coefficient $D_{ss(mig)}$ directly measured by means of the ss migration test (see Eq. (3)) and also to $D_{eff(dif)}$ (see Eq. (4)). In this last case, $D_{ns(dif)}$ has been calculated from the profiles measured after a nss diffusion test (curve fitting by the so-called error function "erf") and the binding capacity $k_d$ has been obtained from these free and total chloride concentration profiles (see Fig. 9a for mortars FA-0 and FA-30 at 90 days, and [48,52,65,72]). Note that, as illustrated in Fig. 9a, the isotherm (expressed in the indicated units) is rather linear within the small chloride concentration range involved in the nss diffusion test, and thus its slope in each point is close to the average value [65]. The comparison between the various methods is presented in Fig. 9b–d, for a broad range of materials. Note that the concretes displayed in Fig. 9c and d do not have systematically the same age. Therefore, in the general case the performances of these concretes cannot be directly compared from these last figures.

Fig. 8 highlights excellent agreement between the two simple methods within the broad range of materials investigated (mortars, as well as concretes with 28-day c.s. from 25 to 87 MPa, with various cements, with or without SCM, and at various ages). This means that both the nss migration test and resistivity measurement provide the same *effective* chloride diffusion coefficients, provided that the effect of the pore solution is taken into account in the "resistivity method": B (see Eq. (7)) depends on the pore solution composition (and thus on W/C). It is therefore not possible to find a single non-empirical formula (*i.e.* not obtained by curve fitting), where *B* is a constant, which can be valid within the whole range of materials. This observation is of importance, since the range of materials available for users is becoming now broader and broader. In addition, Fig. 9 points out that the results obtained by the simple methods ($D_{eff(resistivity)}$ and $D_{eff(mig)} = D_{ns(mig)} \cdot \Phi$) are in agreement with the results provided by direct measurement ($D_{ss(mig)}$) and with $D_{eff(dif)}$ (when available). The differences recorded are quite acceptable with respect to the precision of the

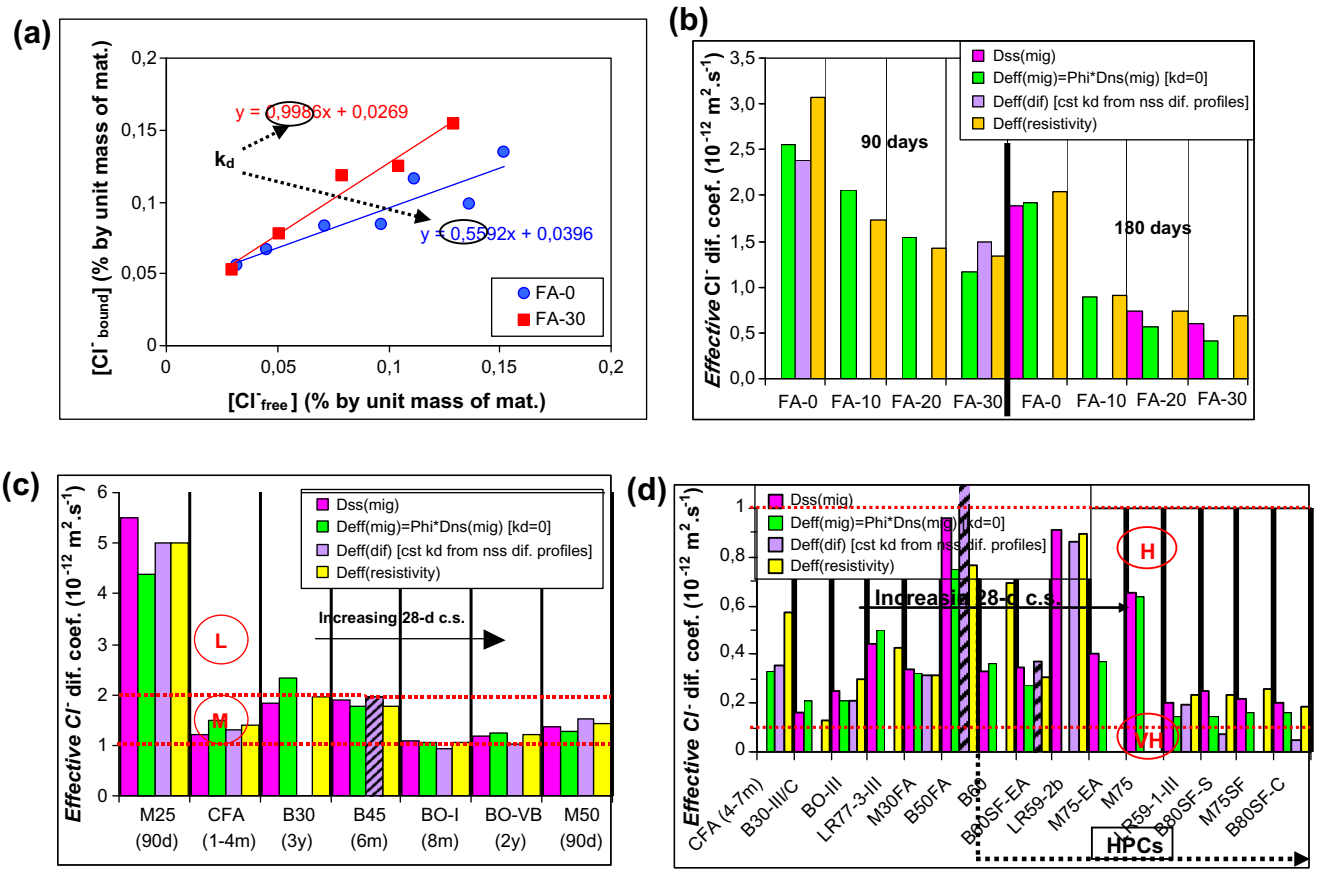


**Fig. 9.** *Effective* chloride diffusion coefficient obtained from ss or nss migration tests, from nss diffusion tests, and from electrical resistivity, on saturated samples, after various water curing periods. *Hatched bars:* $D_{eff(dif)} = 0.16 \cdot D_{ns(dif)}$. *Age is indicated in brackets.* (a) Method of assessment of $k_d$ from concentration profiles. Illustration for mortars FA-0 and FA-30 at 90 days. (b) Mortars (W/B = 0.45 and various FA contents), after 90-day or 180-day water curing. (c) concretes with $D_{eff} \geqslant 1$ (L & M classes). (d) concretes with $D_{eff} < 1$ (H & VH classes).

test methods. The good agreement observed between $D_{eff(mig)} = D_{ns(mig)} \cdot \Phi$ and the other results confirms that very limited binding occurs during nss migration tests and that the assumption $k_d = 0$ is acceptable in most cases. These results indicate in addition that the assessment of the average chloride penetration depth ($x_d$) by the $AgNO_3$ spray test is sufficiently accurate, even in the case of the SCM-concretes tested here.

The assessment *via* the nss diffusion test is significantly more difficult than by the other methods. As a matter of fact, the test is significantly longer, more laborious and more expensive. Moreover, ageing and other chemical effects can affect the results [3,52]. In particular, in the case of concretes with SCMs (more precisely FA), the test can only be used with sufficiently aged materials. Otherwise, as a result of the evolving feature of these materials in the medium term in comparison to the length of the test, $D_{ns(dif)}$ will correspond to a range of ages. Furthermore, the slope of the binding isotherm ($k_d$) has to be calculated from the experimental data for each material by the profile method [72] and this requires the assessment of both the total and the free chloride concentration profiles. Nevertheless, very similar values, whatever the material, have been found here for the coefficient $\Phi \cdot (1 + k_d)$. This means that $k_d$ decreases when $\Phi$ increases, confirming thereby that $k_d$ is related to the C–S–H content of the material and quantifies mainly physical adsorption onto C–S–H, as indicated in [49,73]. A mean value of 0.16 has been calculated here for the range of materials tested. Therefore, a simpler method can be proposed for the assessment of $D_{eff(dif)}$. It consists of measuring one of the chloride concentration profiles (free or total), then assessing the *apparent* coefficient $D_{ns(dif)}$ from it, and using the average fixed value 0.16 to calculate the coefficient $\Phi \cdot (1 + k_d)$ and hence the *effective* chloride diffusion coefficient. Such calculations have been carried out here when experimental values were not available (see hatched bars in Fig. 9). As illustrated in Fig. 9, good agreement is observed between these results and the other methods, thus validating this simplified method based on the nss diffusion test.

Furthermore, excellent agreement has been pointed out in [48,65] between the experimental results obtained by ss migration tests and values predicted by numerical inverse analysis for some of the concretes tested here. The inverse analysis was carried out by means of a numerical multi-species transport model based on the *Nernst–Planck* equation [14,67], where either *Freundlich's* or *Langmuir's* type description was used for the binding isotherm, and from an experimental average chloride penetration depth or total chloride concentration profile, obtained after a nss diffusion test in the lab. This is theoretical confirmation (by means of the multi-species approach and non-linear binding isotherm description) of the validity of the results and of the reliability of the methods described here, based on simplified approaches.

As illustrated in Figs. 8, 9c and d, whatever the method, the class of "potential" durability is the same, except of course when the results are very close to a threshold between classes. In the general case, the values obtained, whatever the method when the age is higher than 90 days, with HPCs, GGBS- and FA-concretes are very small (high or very high "potential" durability). This illustrates again the efficiency of such concretes in reducing chloride

transport. In the case of HPCs, SF incorporation induces a significant decrease in the diffusion coefficient (see Fig. 9d). In the case of CFA (35% FA), FA are not sufficiently beneficial at 1–4 months and a medium "potential" durability is obtained (see Fig. 9c). On the other hand, at 4–7 months, the significant efficiency explains the high "potential" durability recorded (see Fig. 9d). Note that concretes BO-VB, BO-I and M50, with similar mix-compositions (in particular W/C ≈ 0.50), display similar *effective* chloride diffusion coefficients. Fig. 8 points out that $D_{eff}$ of mortar FA-0 (W/C = 0.45) is higher than $D_{eff}$ of plain OPC – CEM I concretes with W/C = 0.48–0.49 at 90 days (see e.g. M50, B50, and LR63-1-EA), confirming that, despite the possible improvement of the mortar matrix by the presence of limestone filler, a lower coefficient is found for concretes compared to this mortar, as usually reported in the literature. This is also consistent with the chloride concentration profiles (see [65]).

## 6. "Intrinsic" liquid water permeability

### 6.1. Definition, significance and methods of assessment

Among the transport properties, the liquid water permeability $k_l{\cdot}k_{rl}(s)$ of a non-saturated medium, where s is the degree of liquid water saturation, $k_l$ the so-called "intrinsic" liquid water permeability (*i.e.* the liquid water permeability of the saturated material) and $k_{rl}$ the relative permeability to liquid ($k_{rl} = 1$ at $s = 1$), governs the (advective) transport of liquid water according to the extended *Darcy's* law. This law characterizes the viscous flow of an incompressible and non-reactive fluid under a total pressure gradient and reads in a one-dimensional scheme along an *x*-axis (see Eq. (13)):

$$v_l = -\frac{k_l}{\eta_l} \cdot k_{rl}(s) \cdot \frac{\partial p_l}{\partial x} \tag{13}$$

where $v_l$ denotes the velocity, $\eta_l$ the dynamic viscosity and $p_l$ the pressure, of liquid water.

The liquid water permeability $k_l{\cdot}k_{rl}$ $(s)$ thus depends on the characteristics of the fluid, on the pore network (pore sizes, connectivity, tortuosity, ...) and on other voids (microcracks, paste-aggregate interfacial zone, ...) of the material, as well as on the moisture state of the sample.

This parameter is of major practical interest even with respect to protection against chloride-induced reinforcement corrosion. As a matter of fact, chloride ingress in tidal zones involves advective transport and is therefore very dependent of the liquid permeability of the material and not only of its chloride diffusion coefficient (see [14,74]). Hence, $k_l$ is required as input data for physical moisture transport or coupled moisture-ion transport models [14,74,81].

Note that in other approaches, specifications [13] or models for SL prediction [82] have been proposed on the basis of the sorptivity [83,84]. Sorptivity is also a relevant parameter, since capillary absorption is the main process, which controls the rate of water (possibly with chlorides, sulphates, ...) ingress in partially saturated conditions. In addition, this parameter can be very easily measured [85]. Consequently, like electrical resistivity, sorptitvity can be regarded as an alternate DI [7]. Nevertheless, this parameter is not a pure transport property. It integrates both transport and moisture equilibrium properties. In addition, it refers to a specific case: absorption in the case of direct contact between an external liquid phase and the surface of the partially saturated sample. Sorptivity can be related to moisture diffusivity in this case [84] and thus to $K_l$ [81].

It is widely admitted that the direct measurement of $k_l$ in the case of low-permeability materials (e.g. HPCs or SCM-mixtures) is difficult [7,83,86] and requires advanced experimental devices (see e.g. [87,88]). With regard to indirect methods, an important work on this topic has been performed by *Scherer* et al. (e.g. rapid methods such as beam bending or thermopermeametry, first applied to gels and later extended to more rigid materials and recently to cement pastes [89]). In the present study, $k_l$ will be inferred from either a *Katz–Thompson* analysis or a numerical inverse analysis of the results from a drying experiment (see following sections).

### 6.2. Assessment of "intrinsic" liquid water permeability $k_l$ by the Katz–Thompson relationship – results and discussion

According to the literature, for some kinds of materials, $k_l$ could be estimated by the *Katz–Thompson* (KT) relationship (analytical law, see Eq. (14)), originally developed for sedimentary rocks and based upon the percolation theory [90,91], when the critical (*i.e.* breakthrough) pore diameter $d_c$ and the formation factor F (see Eq. (6)) of the material are known [44,83,92–95]:

$$k_l = \frac{d_c^2}{226 \cdot F} \tag{14}$$

However, Eq. (14), which relates pore network parameters and transport properties, can be considered as validated only for normal-strength OPC materials, and more particularly for hardened cement pastes [89,92,95]. Hence, the KT relationship has been applied here to various mortars and concretes at various ages, in order to investigate more widely its validity.

Fig. 10 compares the values of $k_l$ obtained by Eq. (14) when *F* is calculated, on the one hand, as the ratio of *effective* chloride diffusion coefficients, and on the other hand, as the ratio of electrical conductivities (see Eq. (6)). The *effective* chloride diffusion coefficient has been assessed by Eq. (3) (ss migration test) or by Eq. (5) (nss migration test and porosity measurement) when ss migration test data were not available. The critical pore diameter $d_c$ has been assessed from MIP measurement (see Section 2.2): $d_c$ is associated with the sudden change in slope observed on the pore volume *vs.* diameter curve. As illustrated in Fig. 10, very good agreement is observed between the $k_l$ values assessed by the two methods of calculation of *F*, as theoretically expected, thus emphasizing the appropriate accuracy of both types of measurement.

Fig. 10b emphasizes that portland cement replacement by 10–30% FA is not sufficiently efficient to decrease $k_l$ at 90 days, contrary to the observations made with $D_{ns(mig)}$ (see Fig. 6). Likewise, *Hedegaard* in 1992 [96] showed by direct measurement the weak efficiency of FA at 28 and 56 days to reduce liquid water permeability (a single FA was tested). On the other hand, the beneficial effect of FA on $k_l$ at 180 days is obvious from 10% FA (see Fig. 10b) and is in agreement with the literature (direct measurement [30]). As a matter of fact, as chemical reactions progress, permeability will be significantly reduced once the connectivity of the large-size (e.g. capillary) void network will be significantly reduced. On the other hand, $D_{ns(mig)}$ will be rapidly affected by the presence of FA for the various reasons explained in Sections 1 and 4.2 (e.g. physical and chemical interactions, as well as pore blocking induced by solid "islands" formed by additional C–S–H within the range involved in ionic diffusion). These findings were at least partly expected from the MIP data: for example Fig. 4a indicates that the FA-30 capillary pore structure has drastically changed between 90 and 180 days (see also [34]).

Contrary to Fig. 8 ($D_{eff}$), Fig. 10 points out the efficiency of the (FA-0) mortar matrix to decrease $k_l$: the $k_l$ value is lower than the values recorded for plain OPC – CEM I concretes even with lower W/C (see e.g. B55 (W/C = 0.41) and LR69-1-EA (W/C = 0.43)).

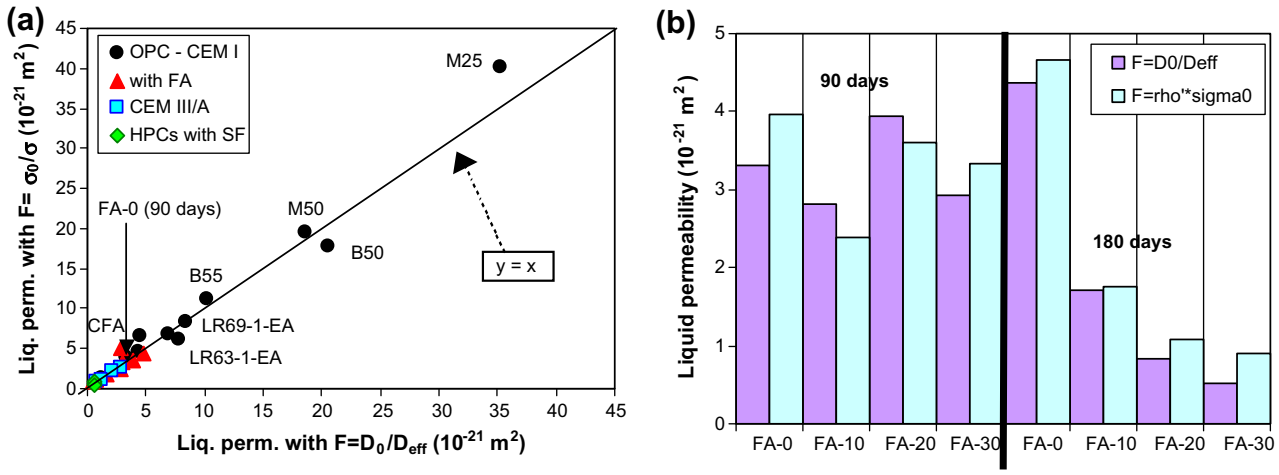


**Fig. 10.** Comparison between two methods of calculation of the "intrinsic" liquid water permeability $k_l$ by using the *Katz–Thompson* relationship. *Age is indicated in brackets.* (a) Concretes and mortars, at various ages. (b) Mortars (W/B = 0.45 and various FA contents), after 90-day or 180-day water curing.

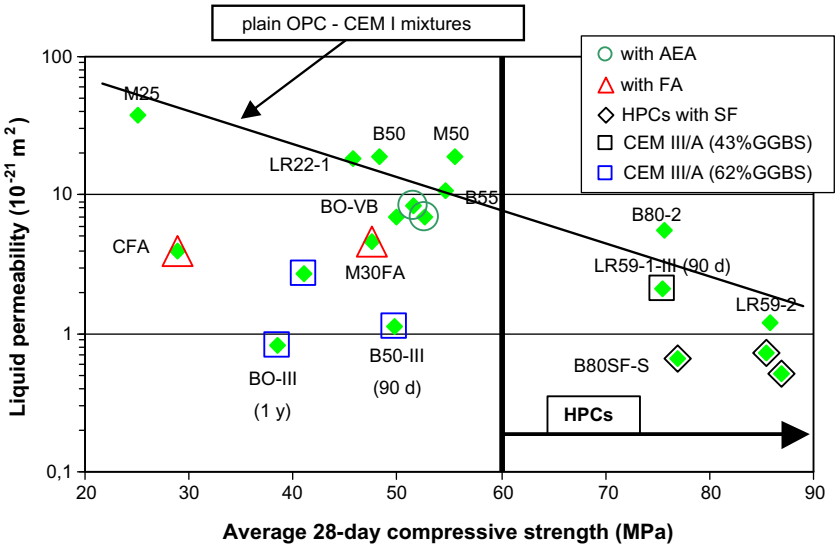


**Fig. 11.** Mean values of "intrinsic" liquid water permeability $k_l$ assessed by the *Katz–Thompson* relationship *vs.* the average 28-day cylinder c.s., for various concretes and ages. *Age is indicated in brackets.*

All of these results confirm that permeability and diffusion coefficients provide complementary information with regard to durability, as already pointed out in [3,7,34], and justify the selection of both parameters as DIs.

Fig. 11 depicts the values of $k_l$ (average values of the two methods of calculation of *F*, except for LR22-1 where no resistivity value was available) assessed by the KT relationship *vs.* the average 28-day cylinder c.s. of the concrete. Fig. 11 exhibits the range of $k_l$ values obtained by this method when the 28-day c.s. ranges from 25 to 87 MPa. Whatever the age ($\geqslant$90 days), normal-strength 62%-GGBS concretes are revealed to be almost as efficient as SF-HPCs to reach very low "intrinsic" liquid water permeabilities. These $k_l$ values are at least one order of magnitude lower than that of plain OPC – CEM I concretes with the same 28-day c.s.

### 6.3. Assessment of "intrinsic" liquid water permeability $k_l$ by numerical inverse analysis – comparison with the Katz–Thompson relationship

In order to verify the validity of the empirical KT relationship to assess the "intrinsic" liquid water permeability $k_l$ of concretes, a comparison has been carried out with a more sophisticated but more theoretical method. This is an indirect method (based on inverse analysis), which combines experiments and a numerical model. This method, initially proposed by *Coussy* et al. [97], is based on the analysis of the relative mass loss *vs.* time plots (kinetics) obtained in the course of a drying test at a given relative humidity (RH) and at constant temperature [52]. In the general case, it requires an advanced isothermal moisture transport model, which involves the transport of liquid water and gas according to the extended *Darcy's* law and the relative diffusion of water vapour (and dry air) with respect to the gas mixture governed by *Fick's* first law, with non-constant total gas pressure [81]. In addition, the model requires the assessment of the porosity and the water vapour desorption isotherm [52,81]. Moreover, the initial moisture state has to be known. It usually corresponds to almost saturated conditions ($s \approx 1$). $k_l$ is hence deduced from the best fitting of the drying kinetics predicted by the model on the values observed for the sample submitted to the drying test (e.g. exposure to RH = 54% for 6 months, see Fig. 12a).

This method has been applied here to different types of concretes. The results obtained are compared in Fig. 12b to the

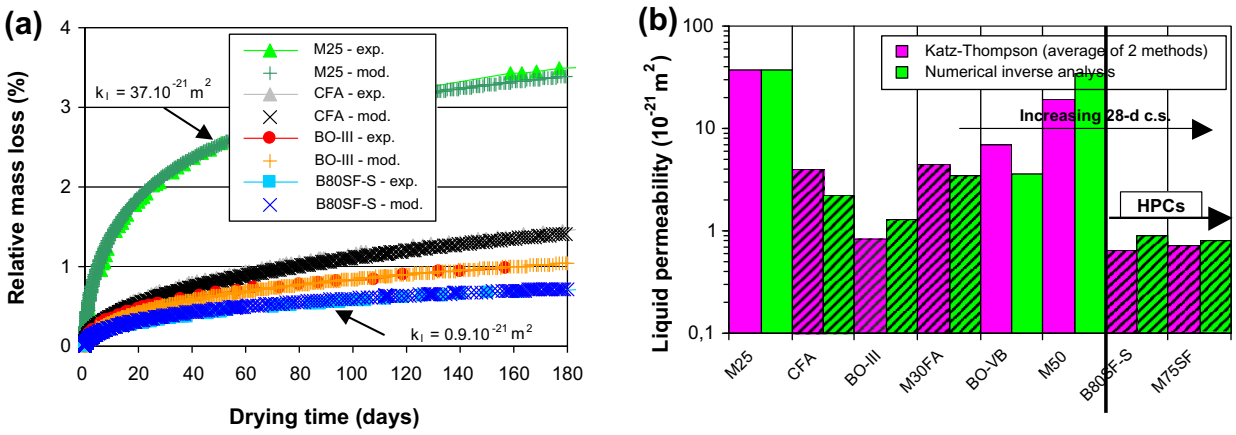


**Fig. 12.** "Intrinsic" liquid water permeability $k_l$ assessed by numerical inverse analysis from drying kinetics. (a) Illustration of the method of assessment for five types of concretes: fitting of drying kinetics of samples submitted to RH = 54% and to $T = 21 \pm 1$ °C for 6 months after 1- or 2-year water curing and saturation. (b) comparison with the *Katz–Thompson* relationship, for various concretes and ages. *Hatched bars: SCM–concretes.*

results obtained by the *KT* relationship (average values of the two methods of calculation of *F*, see Section 6.2) for various concretes (28-day c.s. from 25 to 85 MPa) and ages. Fig. 12b points out that the results provided by the simple empirical method (*KT* relationship) are quite consistent with the theoretical computations (numerical inverse analysis) based on completely different tests, for the various concretes considered. This confirms the relevance and the validity of the *KT* relationship to assess the "intrinsic" liquid water permeability of concretes, even in the presence of SCMs. Of course, in order to further validate the method, comparison with direct "intrinsic" liquid water permeability measurement should be made. Note that, when the mentioned numerical model (or a simplified one [52,97]) and the required input data are available, the method based on inverse analysis has also the advantage of requiring a single simple (drying) experiment, which does not need any specific apparatus and which can be carried out easily in every lab.

M30FA (30% FA) and BO-III (62% GGBS) have been tested here at the same age (1 year) and have the same W/B. It can be seen in Fig. 12b that despite its lower 28-day c.s. (see Table 1), BO-III exhibits a lower $k_l$ value than M30FA, thus pointing out the better efficiency of 62% GGBS than 30% FA for reducing $k_l$.

## 7. Conclusion

Different methods for assessing, on the one hand the *effective* chloride diffusion coefficient $D_{eff}$, and on the other hand the "intrinsic" liquid water permeability $k_l$, of saturated materials have been compared in this paper on a set of water-cured materials ranging from low-grade to high-performance concretes. The very good agreement observed in each case points out the validity and the reliability of the proposed methods. More precisely, $D_{eff}$ can be assessed from resistivity measurement, ss migration test, nss migration test and nss diffusion test (and numerical inverse analysis [48,65]). Likewise, $k_l$ can be assessed from the *Katz–Thompson* relationship, as well as from numerical inverse analysis from drying kinetics. The application of the "resistivity method" is a little more complicated for high-porosity plain OPC – CEM I concretes. Difficulties can also be exhibited in nss migration (or diffusion) tests with dense or high-volume GGBS concretes. Nevertheless, simple and rapid test methods can allow assessment of durability indicators with sufficient accuracy in the general case. An advanced statistically-based investigation of the precision of the lab tests for a broad range of materials remains to be done, as well as direct measurement of $k_l$, in order to finalize the evaluation of the methods.

The specificities of the behaviour of SCM-mixtures have been pointed out. As expected, good durability-related properties have been pointed out for mature concretes made with CEM III/A (62% GGBS) or with FA (20–35%). The transport properties (*apparent* and *effective* chloride diffusion coefficients, as well as "intrinsic" liquid water permeability) of such normal-strength concretes can be close to that of HPCs with SF, even if the porosity is not very low. Nevertheless, the results have also enhanced the more marked and determining ageing effect associated with these materials (in particular with FA), and this is emphasized in the case of $k_l$. As a matter of fact, significantly better properties are recorded at later ages, after water curing, within the range investigated here, and hence very different DI values can be measured, depending on the age. For example with the mortars tested here (10–30% FA), even if the FA beneficial effect is exhibited on the *apparent* chloride diffusion coefficient from 90 days, FA are revealed as beneficial only at 180 days with regard to $k_l$. This confirms the usefulness and the complementary nature of these two DIs to assess the "potential" durability related to reinforcement corrosion. Furthermore, no improvement has been recorded in the *apparent* and *effective* chloride diffusion coefficients for the 39%-FA concrete tested here even at 180 days.

In field conditions, the beneficial effect of FA or GGBS can be compromised (as a result of early-age drying, early exposure to aggressive species, carbonation, skin effect, ...) and will markedly depend on the curing and environmental conditions, since such SCM-materials (in particular FA-materials) are very sensitive to these conditions. This has been illustrated for example within the framework of the BHP 2000 French National Project [33] in a study carried out both in the lab and in various outdoor environments on some of the concretes investigated here. Therefore, it is particularly important to investigate the behaviour both in lab and field conditions in the case of concretes with high volumes of SCM. First it is of importance to perform lab tests at 90 days and even at 180 days, in order to, on the one hand characterize the bulk concrete properties, and on the other hand avoid errors and variability associated with lab tests due to ageing effects. In addition, it is necessary to account for early-age behaviour, which will characterize the "covercrete" of the structure.

The methods and the corresponding results on various types of materials presented in this paper can be useful to assist engineers in selecting a reliable methodology to assess DIs and carry out durability assessment or prediction. In particular, the data

displayed in the paper can provide helpful references when testing new materials or searching to meet durability criteria. The values can also be used as input data in predictive models for similar mixtures as those tested in this study, thus allowing one to avoid long lab tests before implementation of the model. A performance-based approach using a set of relevant and complementary DIs, along with the simple methods discussed here to assess these DIs, can constitute a useful tool to address the durability of new materials, to quantify the actual benefit of SCMs on medium-term and long-term durability, and more generally to perform concrete mix-design for a predefined durability. This will help in the development of new (high-tech) and green solutions within the framework of sustainable development.

## Acknowledgements

The authors gratefully acknowledge P. Belin, J.F. Bouteloup, L. Routhe and X. Wang (LCPC, Paris, France), as well as the LRPCs of Clermont-Ferrand (B. Boulet), Est Parisien (C. Mallet), Lille (J.J. Brioist), Lyon (M. Dierkens), and Saint-Brieuc (B. Thauvin), for their contribution to the experiments and their involvement in the LPC research project *"Performance-based and probabilistic durability approach"*.

## References

[1] Aïtcin PC. Cement and concrete development from an environmental perspective. In: Proc. Int. Workshop "Concrete Technology for a sustainable development in the 21st century", Lofoten Islands, Norway; June 1998.
[2] Lukasik J, Damtoft JS, Herfort D, Sorrentino D, Gartner EM. Sustainable development and climate changes initiatives. In: Beaudoin JJ, Makar J, Raki L, editors. Montréal, 2007. Proceedings of the 12th international congress on the chemistry of cement (ICCC 2007), Montréal, Québec, Canada, July 8–13, 2007.
[3] Baroghel-Bouny V. Development of a global, performance and predictive approach of durability of (reinforced) concrete structures on the basis of durability indicators – results and perspectives. Characterization of the microstructure of concretes, study of their moisture and transport properties, assessment of free deformations and service life prediction (in French), LPC studies and researches, OA 63 (LCPC, Paris, 2008), 311 p.
[4] Leboullenger B. Account for global cost in the construction field in public policies. Methodological considerations (in French). In: Proc. AFGC Technical Seminar "Cycle de vie des ouvrages: une approche globale (GC'2009)", Cachan, France; 18–19 March 2009.
[5] EN 206-1 – concrete – part 1: specification, performance, production and conformity, CEN, December 2000.
[6] FIB 2006 – model code for service life design, FIB Bulletin, vol. 34; 2006. 110 p.
[7] Baroghel-Bouny V, et al. Concrete design for a given structure service life – durability management with regard to reinforcement corrosion and alkali-silica reaction. State-of-the-art and guide for the implementation of a predictive performance approach based upon durability indicators, AFGC Scientific and Technical Documents (AFGC, Paris, issue in French: 2004, issue in English: 2007), 240 p.
[8] Baroghel-Bouny V. Durability indicators: relevant tools for an improved assessment of RC durability. In: Toutlemonde F, Sakai K, Gjørv OE, Banthia N, editors. LCPC, 2007. Proc. 5th int. conf. on concrete under severe conditions: environment and loading (CONSEC'07), June 4–6, 2007, vol. 1, Tours, France, pp. 67–84.
[9] Baroghel-Bouny V. Durability indicators: relevant tools for performance-based evaluation and multi-level prediction of RC durability. In: Baroghel-Bouny V, Andrade C, Torrent R, Scrivener K, editors. Proc. int. RILEM workshop on performance based evaluation and indicators for concrete durability, March 19–21, 2006, Madrid, Spain. Bagneux: RILEM Publ. 2007. PRO 47, 3–30.
[10] Andrade C, Alonso C, Arteaga A, Tanner P. Methodology based on the electrical resistivity for the calculation of reinforcement service life. L'industria Italiana del cemento 2001;764:330–9.
[11] Du Preez AA, Alexander MG. A site study of durability indexes for concrete in marine conditions. Mater Struct 2004;37(267):146–54.
[12] Baroghel-Bouny V, Andrade C, Torrent R, Scrivener K, editors. Proc int RILEM workshop on performance based evaluation and indicators for concrete durability, March 19–21, 2006, Madrid, Spain. Bagneux: RILEM Publ.; 2007, PRO 47.
[13] Alexander MG, Ballim Y, Stanish K. A framework for use of durability indexes in performance-based design and specifications for reinforced concrete structures. Mater Struct 2008;41:921–36.
[14] Baroghel-Bouny V, Nguyen TQ, Dangla P. Assessment and prediction of RC structure service life by means of durability indicators and physical/chemical models. Cem Concr Compos 2009;31(8):522–34.
[15] Thiery M, Cremona C, Baroghel-Bouny V. Application of the reliability theory to the assessment of the carbonation-induced corrosion risk of rebars. Euro J Environ Civil Eng 2011, accepted for publication.
[16] Atkins M, Glasser FP. Application of Portland cement-based materials to radioactive waste immobilisation. J Waste Manage 1992;12:105–31.
[17] Thomas MDA, Shehata MH, Shashiprakash SG, Hopkins DS, Cail K. Use of ternary cementitious systems containing silica fume and fly ash in concrete. Cem Concr Res 1999;29:1207–14.
[18] Bilodeau A, Malhotra VM. High-volume fly ash system: concrete solution for sustainable development. ACI Mater J 2000;97(1):41–9.
[19] Bleszynski R, Hooton RD, Thomas MDA, Rogers CA. Durability of ternary blend concrete with silica fume and blast-furnace slag: laboratory and outdoor exposure site studies. ACI Mater J 2002;99(5):499–508.
[20] Naik TR, Ramme BW, Kraus RN. Durability of concrete with high-volumes of fly ash. In: Sato R, Fujimoto Y, Dohi T editors. Proc. int. seminar on durability and lifecycle evaluation of concrete structures – 2004, September 13, 2004, Higashi-Hiroshima, Japan. Univ. of Hiroshima; 2004.
[21] Larbi JA, Fraay ALA, Bijen JM. The chemistry of the pore fluid of silica fume-blended cement systems. Cem Concr Res 1990;20:506–16.
[22] Richardson IG. The nature of C–S–H in hardened cements. Cem Concr Res 1999;29:1131–47.
[23] Li S, Roy DM. Investigation of relations between porosity, pore structure, and $Cl^-$ diffusion of fly ash and blended cement pastes. Cem Concr Res 1986;16:749–59.
[24] Villain G, Baroghel-Bouny V, Kounkou C. Comparative study of the induced hydration, drying and deformations of self-compacting and ordinary mortars. In: Skarendahl A, Petersson O, editors. Proc 1st int RILEM symp "self-compacting concrete", September 13–17, 1999, Stockholm, Sweden. RILEM, Paris; 1999. PRO 7. p. 131–42.
[25] Ngala VT, Page CL, Parrott LJ, Yu SW. Diffusion in cementitious materials: II. Further investigations of chloride and oxygen diffusion in well-cured OPC and OPC/30% PFA pastes. Cem Concr Res 1995;25(4):819–26.
[26] Zhang T, Gjørv OE. Diffusion behavior of chloride ions in concrete. Cem Concr Res 1996;26(6):907–17.
[27] Amiri O, Aït-Mokhtar A, Dumargue P, Touchard G. Electrochemical modelling of chloride migration in cement based materials. Part I: theoretical basis at microscopic scale. Electrochem Acta 2001;46:1267–75.
[28] Page CL, Vennesland O. Pore solution composition and chloride binding capacity of silica-fume cement pastes. Mater Struct 1983;16(91):19–25.
[29] Hornain H, Thuret B, Guedon-Dubied S, Le Roux A, Laporte F. Pigeon M, et al. Influence of aggregates and mineral additives on the composition of the pore solution. In: Shayan A, editor. Proc. 10th ICAARC, Melbourne, Australia; August 18–23, 1996. p. 514–21.
[30] Hussain SE, Rasheeduzzafar. Corrosion resistance performance of fly ash blended cement concrete. ACI Mater J 1994;91(3):264–72.
[31] De Larrard F, Baroghel-Bouny V. Ageing of concrete in natural environments: an experiment for the 21st century. I – general considerations and initial mechanical properties of tested concrete (in French). Bull Lab Ponts Chaus 2000:51–65.
[32] Arliguie G, Hornain H, editors. "GranDuBé – Grandeurs associées à la durabilité des bétons (durability-related parameters)" (in French). RGCU – AFGC – Presses de l'ENPC, Paris; April 2007, p. 63–106.
[33] Baroghel-Bouny V, Gawsewitch J, Belin P, Ounoughi K, Arnaud S, Olivier G, et al. Ageing of concrete in natural environments: an experiment for the 21st century. IV – results on cores extracted from field-exposed test specimens of various sites as part of the first measurement sequence. Bull Lab Ponts Chaus 2004;249:49–100.
[34] Kinomura K, Baroghel-Bouny V. Pore Structure and transport properties of high-volume fly ash materials used for radioactive waste disposal facilities. In: Proc int RILEM workshop "Long-Term performance of cementitious barriers and reinforced concrete in nuclear power plants and waste management (NUCPERF 2009)", Cadarache, France; 30 March–02 April 2009.
[35] Andrade C, d'Andréa R. Electrical resistivity as microstructural parameter for the calculation of reinforcement service life. In: Proc int conf on microstructure related durability of cementitious composites, Nanjing, China; October 13–15, 2008.
[36] Polder RB. Test methods for on site measurement of resistivity of concrete – A RILEM TC-154 technical recommendation. Constr Build Mater 2001;15(2–3):125–31.
[37] Frederiksen JM, Sorensen HE, Andersen A, Klinghoffer O. The effect of the W/C ratio on chloride transport into concrete. In: Frederiksen V, editor. Immersion, migration and resistivity tests, HETEK Report n° 54. Danish Road Directorate, Copenhagen; 1997.
[38] Kyi AA, Batchelor B. An electrical conductivity method for measuring the effects of additives on effective diffusivities in portland cement pastes. Cem Concr Res 1994;24(4):752–64.
[39] Tuutti K. Corrosion of steel in concrete. Report 4.82, Swedish Cem Conc Res Inst (CBI), Stockholm, Sweden; 1982.
[40] Belin P. Baroghel-Bouny V. Measurement of electrical resistivity of saturated concrete: development of a test method (in French). Research Project 11B021 "Durability of reinforced concrete and of its constituents: control and performance-based approach", Research Report, LCPC; May 2006, 18 p + annexes.
[41] Newlands MD, Jones MR, Kandasami S, Harrison TA. Sensitivity of electrode contact solutions and contact pressure in assessing electrical resistivity of concrete. Mater Struct 2008;41(4):621–32.

[42] ChlorTest – EU funded research project G6RD-CT-2002-0085 "Resistance of concrete to chloride ingress – From laboratory tests to in-field performance", WP 5 report – final evaluation of the test methods, prepared by Tang Luping, Deliverables D16-19; 2005. 38 p.
[43] Castellote M, Andrade C. Round-Robin Test on methods for determining chloride transport parameters in concrete, RILEM technical committee. Mater Struct 2006;39(10):955–90.
[44] Garboczi EJ. Permeability, diffusivity and microstructural parameters: a critical review. Cem Concr Res 1990;20(4):591–601.
[45] Cabrera JG, Ghoddoussi P. The influence of fly ash on the resistivity and rate of corrosion of reinforced concrete. In: Proc. 4th CANMET/ACI int conf on concrete durability, Nice, France; 1994, SP-145. p. 229–44.
[46] Tumidajski P, Schumacher A, Perron S, Gu P, Beaudoin J. On the relationship between porosity and electrical resistivity in cementitious systems. Cem Concr Res 1996;26(4):539–44.
[47] Thiery M. Modelling of atmospheric carbonation of cementitious materials. Account for kinetic effects as well as microstructure and moisture changes (in French), Etudes et Recherches des LPC, OA 52. LCPC, Paris; 2006. 337 p.
[48] Baroghel-Bouny V, Belin P, Maultzsch M, Henry D. $AgNO_3$ spray tests – advantages, weaknesses, and various applications to quantify chloride ingress into concrete. Part 2: non-steady-state migration tests and chloride diffusion coefficients. Mater Struct 2007;40(8):783–99.
[49] Tang L. Chloride transport in concrete – measurement and prediction, PhD thesis, Publ. P-96:6, Depart of Building Materials, Chalmers Univ of Technology, Göteborg, Sweden; 1996. 461 p.
[50] Tang L, Nilsson LO. Rapid determination of the chloride diffusivity in concrete by applying an electrical field. ACI Mater J 1992;89(1):49–53.
[51] NT Build 492: Nordtest method, concrete, mortar and cement-based repair materials: chloride migration coefficient from non-steady-state migration experiments, Espoo, Finland; 1999.
[52] Baroghel-Bouny V, Thiery M, Barberon F, Coussy O, Villain G. Assessment of transport properties of cementitious materials: a major challenge as regards durability? Euro Rev Civil Eng 2007;11(6):671–96.
[53] Wiens U. Zur wirkung von steinkohlenflugasche auf die chloridinduzierte korrosion von stahl in beton (in German), PhD thesis, Technische Hochschule, Fachbereich 3, Aachen, 2004. In: Schriftenreihe des Deutschen Ausschusses für Stahlbeton, Berlin, Nr. 551; 2005. 214 p.
[54] Lu X. Application of the Nernst–Einstein equation to concrete. Cem Concr Res 1997;27(2):293–302.
[55] Papadakis VG. Effect of supplementary cementing materials on concrete resistance against carbonation and chloride ingress. Cem Concr Res 2000;30:291–9.
[56] Alexander MG, Mackechnie JR. Predictions of long-term chloride ingress from marine exposure trials. In: Hooton RD, Thomas MDA, Marchand J, Beaudoin JJ, editors. Materials science of concrete, special vol.: ion and mass transport in cement-based materials. Skalny JP, series editor. Am Ceram Soc. Westerville; 2001. p. 281–91.
[57] Mohammed TU, Yamaji T, Hamada H. Chloride diffusion, microstructure, and mineralogy of concrete after 15 years of exposure in tidal environment. ACI Mater J 2002;99(3):256–63.
[58] Thomas MDA, Matthews JD. Performance of pfa concrete in a marine environment - 10-year results. Cem Concr Compos 2004;26(1):5–20.
[59] Saillio M, Barberon F, Baroghel-Bouny V, Gegout P, Platret G, D'Espinose de la Caillerie JB. Interactions between chloride ingress and carbonation in cementitious materials. In: Proc. XIII$^{h}$ int. congress on the chemistry of cement "cementing a sustainable future" (ICCC 2011), Madrid, Spain; July 3–8, 2011.
[60] Edvardsen C, Jepsen MT. Chloride migration coefficients from non-steady-state migration experiments at environment-friendly "green" concrete. In: Andrade C, Kropp J, editors. Proc. 2nd int. RILEM workshop "testing and modelling chloride ingress into concrete" RILEM, Paris, France, PRO 19, 203-209; September 11–12, 2000.
[61] Dhir RK, Jones MR. Development of chloride-resisting concrete using fly ash. Fuel 1999;78:137–42.
[62] Page CL, Short NR, El Tarras A. Diffusion of chloride ions in hardened cement paste. Cem Concr Res 1981;11:395–406.
[63] Dhir RK, El-Mohr MAK, Dyer TD. Chloride binding in GGBS concrete. Cem Concr Res 1996;26(12):1767–73.
[64] Luo R, Cai Y, Wang C, Huang X. Study of chloride binding and diffusion in GGBS concrete. Cem Concr Res 2003;33(1):1–7.
[65] Baroghel-Bouny V., Wang X., Thiery M., Prediction of chloride binding isotherms by analytical model or numerical inverse analysis. In: van Breugel K, Ye Guang, Yuan Yong, editors. Proc 2nd int symp on service life design for infrastructures, October 4–6, 2010, Delft, The Netherlands, vol. 1. RILEM Publ., Bagneux; 2010, PRO 70. p. 513–26.
[66] Samson E, Marchand J, Snyder KA. Calculation of ionic diffusion coefficients on the basis of migration test results. Mater Struct 2003;36:156–65.
[67] Nguyen TQ, Baroghel-Bouny V, Dangla P. Prediction of chloride ingress into saturated concrete on the basis of a multi-species model by numerical calculations. Compos Concr 2006;3(6):401–22.
[68] Andrade C. Calculation of chloride diffusion coefficients in concrete from ionic migration measurements. Cem Concr Res 1993;23(3):724–42.
[69] Andrade C, Sanjuan MA. Experimental procedure for the calculation of chloride diffusion coefficients in concrete from migration tests. Adv Cem Res 1994;6(23):127–34.
[70] Castellote M, Andrade C, Alonso C. Measurement of the steady and non-steady state chloride diffusion coefficients in a migration test by means of monitoring the conductivity in the anolyte chamber. Comparison with natural diffusion tests. Cem Concr Res 2001;31(10):1411–20.
[71] Truc O, Ollivier JP, Carcasses M. A new way for determining the chloride diffusion coefficient in concrete from steady state migration tests. Cem Concr Res 2000;30(2):217–26.
[72] Baroghel-Bouny V, Belin P, Castellote M, Rafaï N, Rougeau P, Yssorche-Cubaynes MP. Which toolkit for durability evaluation as regards chloride ingress into concrete? Part I: comparison between various methods for assessing the chloride diffusion coefficient of concrete in saturated conditions. In: Andrade C, Kropp J, editors. 3$^{rd}$ Int RILEM workshop "testing and modelling chloride ingress into concrete", September 9–10, 2002, Madrid, Spain. Bagneux: RILEM Publ.; 2004. PRO 38. p. 105–36.
[73] Tang L, Nilsson LO. Ionic migration and its relation to diffusion. In: Hooton RD, Thomas MDA, Marchand J, Beaudoin JJ, editors. Skalny JP, series editor. Materials science of concrete, special vol.: "Ion and mass transport in cement-based materials". Am Ceram Soc, Westerville; 2001. p. 81–96.
[74] Baroghel-Bouny V, Thiery M, Wang X. Modelling of isothermal coupled moisture-ion transport in cementitious materials. Cem Concr Res 2011, doi:10.1016/j.cemconres.2011.04.001.
[75] Castellote M, Andrade C, Alonso C. Chloride-binding isotherms in concrete submitted to non-steady-state migration experiments. Cem Concr Res 1999;29:1799–806.
[76] Dullien FAL. Porous media. Fluid transport and pore structure. Academic Press; 1979.
[77] Rajabipour F, Weiss J. Electrical conductivity of drying cement paste. Mater Struct 2007;40(12):1143–60.
[78] Tong L, Gjorv OE. Chloride diffusivity based on migration testing. Cem Concr Res 2001;31:973–82.
[79] Koryta J, Dvorak J. Principles of electrochemistry. John Wiley & Sons; 1987.
[80] Atkins PW. Physical chemistry. 4th ed. Oxford: Oxford Univ. Press; 1990.
[81] Thiery M, Baroghel-Bouny V, Bourneton N, Villain G, Stefani C. Modelling of drying of concrete - analysis of the different moisture transport modes (in French). Euro Rev Civil Eng 2007;11(5):541–77.
[82] Bentz DP, Ehlen MA, Ferraris CF, Garboczi EJ. Sorptivity-based service life predictions for concrete pavements. In: Proc. 7th int conf on concrete pavements, vol. 1. September 9–13, 2001, Orlando, Florida. Int Soc Conc Pavements; 2001. p. 181–93.
[83] Martys NS. Survey of concrete transport properties and their measurement. NIST Report NISTIR 5592; 1995. 40 p.
[84] Lockington D, Parlange J, Dux P. Sorptivity and the estimation of water penetration into unsaturated concrete. Mater Struct 1999;32(5):342–7.
[85] ASTM C1585-04 – standard test method for measurement of rate of absorption of water by hydraulic-cement concrete. ASTM International; 2004.
[86] Perraton D, Aïtcin PC, Carles-Gibergues A. Permeability, as seen by the researcher. In: Malier Y, E, Spon FN, editors. High performance concrete – from material to structure. Cambridge (UK): Chapman & Hall; 1992. p. 252–75.
[87] Hearn N, Mills RH. A simple permeameter for water or gas flow. Cem Concr Res 1991;21(2/3):257–61.
[88] El-Dieb AS, Hooton RD. A high pressure triaxial cell with improved measurement sensitivity for saturated water permeability of high performance concrete. Cem Concr Res 1994;24(5):854–62.
[89] Scherer GW, Valenza II JJ, Simmons G. New methods to measure liquid permeability in porous material. Cem Concr Res 2007;37(3):386–97.
[90] Katz AJ, Thompson AH. Quantitative prediction of permeability in porous rock. Phys Rev B 1986;34(11):8179–81.
[91] Thompson AH, Katz AJ, Krohn CE. The microgeometry and transport properties of sedimentary rocks. Adv Phys 1987;36(5):625–93.
[92] El-Dieb AS, Hooton RD. Evaluation of the Katz–Thompson model for estimating the water permeability of cement-based materials from mercury intrusion porosimetry data. Cem Concr Res 1994;24(3):443–55.
[93] Halamickova P, Detwiler RJ, Bentz DP, Garboczi EJ. Water permeability and chloride ion diffusion in portland cement mortars: relationship to sand content and critical pore diameter. Cem Concr Res 1995;25(4):790–802.
[94] Christensen BJ, Mason TO, Jennings HM. Comparison of measured and calculated permeabilites for hardened cement pastes. Cem Concr Res 1996;26(9):1325–34.
[95] Tumidajski PJ, Lin B. On the validity of the Katz–Thompson equation for permeabilities in concrete. Cem Concr Res 1998;28(5):643–7.
[96] Hedegaard SE, Hansen TC. Water permeability of fly ash concretes. Mater Struct 1992;25:381–7.
[97] Coussy O, Baroghel-Bouny V, Dangla P, Mainguy M. Assessment of the water permeability of concretes from their mass loss during drying (in French). Rev Fran Génie Civil 2001;5(2–3):269–84.